ORGANOMETALLICS
Article

Organometallics **2010,** *29,* 6711–6722 6711
DOI: 10.1021/om100732d

Activation of an Aryl C−H Bond Converts Chelating Diphenolate Ligands Bound to Zirconium into Trianionic Pincer Ligands: σ-Donor Ligand Effects versus Thermolysis

Subramaniam Kuppuswamy, Ion Ghiviriga, Khalil A. Abboud, and Adam S. Veige*

Center for Catalysis, University of Florida, P.O. Box 117200, Gainesville, Florida 32611, United States

Received August 6, 2010

This report describes the synthesis and characterization of new zirconium benzyl complexes supported by a trianionic pincer ligand. Treating $Zr(CH_2Ph)_4$ with the terphenyldiol [^{t}BuOCO]H_3 (**1**) in benzene affords [^{t}BuOCHO]$Zr(CH_2Ph)_2$ (**2**). Thermolysis of **2** leads to formation of dinuclear {[^{t}BuOCO]$ZrCH_2Ph$}$_2$ (**3**), which contains a five-coordinate zirconium center in a trigonal-bipyramidal (tbp) geometry. Adding 2 equiv of PMe_3 to **2** affords [^{t}BuOCO]$ZrCH_2Ph(PMe_3)_2$ (**4-PMe$_3$**). X-ray crystallographic analysis reveals strong agostic interactions for the benzyl ligand in both **3** and **4-PMe$_3$**. Treatment of **2** with 2 equiv of THF results in hydrocarbon-soluble [^{t}BuOCO]$ZrCH_2Ph(THF)_2$ (**5**). NMR spectroscopic measurements indicate a C_{2v}-symmetric molecule that is isostructural with **4-PMe$_3$**. Addition of the larger phosphine PMe_2Ph to **2** provides the corresponding mono-PMe_2Ph complex in solution, but a small amount of the bis-diphenolate [^{t}BuOCHO]$_2$Zr (**6**) also forms. Complex **6** was independently synthesized by treating $Zr(CH_2Ph)_4$ with 2 equiv of **1**. When 2 equiv of pyridine (py) is added to **2**, the intermediate [^{t}BuOCHO]$ZrCH_2Ph(\eta^2-C_5H_4N)$py (**7**) results from pyridine *o*-C−H bond activation. After 48 h, complex **7** releases another 1 equiv of toluene by activation of the pincer C_{ipso}−H bond to produce the trianionic pincer complex [^{t}BuOCO]$Zr(\eta^2-C_5H_4N)(py)_2$ (**8**). Multinuclear and 2D NMR spectroscopic experiments and combustion analysis support the molecular assignment of **8**. Addition of α-picoline to **2** provides different results compared to py. Initially, the α-picoline adduct [^{t}BuOCHO]$Zr(CH_2Ph)_2$(α-picoline) (**9**) forms. Addition of another 1 equiv of α-picoline provides the mixed η^2(*N,C*)-6-Me-pyridyl)/η^2(*N,C*-CH_2)-pyrid-2-yl complex [^{t}BuOCHO]$Zr(\eta^2$(*N,C*)-6-Me-pyridyl)(η^2(*N,C*-CH_2)-pyrid-2-yl) (**10**).

Introduction

Electronically unsaturated, neutral four-coordinate zirconium monoalkyl or hydride species are important intermediates in numerous transformations, including hydrozirconation,[1−5] hydrosilylation,[6] olefin polymerization,[7−12] and hydrogenolysis of alkanes[13−16] and polyolefins.[12,17] More recently, their application was extended to the dehydrocoupling of phosphines[18−20] and arsines[21] and heterocoupling of phosphines with silanes and germanes.[22,23] Trianionic pincer ligands[7,24−32] fuse three anionic donor groups, providing nearly exclusive meridional

*To whom correspondence should be addressed. E-mail: veige@chem.ufl.edu.

(1) Wipf, P.; Kendall, C. *Top. Organomet. Chem.* **2004**, *8*, 1.
(2) Schwartz, J.; Labinger, J. A. *Angew. Chem., Int. Ed.* **1976**, *15*, 333.
(3) Hart, D. W.; Schwartz, J. *J. Am. Chem. Soc.* **1974**, *96*, 8115.
(4) Wailes, P. C.; Weigold, H.; Bell, A. P. *J. Organomet. Chem.* **1972**, *43*, C32.
(5) Wailes, P. C.; Weigold, H. *J. Organomet. Chem.* **1970**, *24*, 405.
(6) Jia, L.; Zhao, J. Q.; Ding, E.; Brennessel, W. W. *Dalton Trans.* **2002**, 2608.
(7) Golisz, S. R.; Bercaw, J. E. *Macromolecules* **2009**, *42*, 8751.
(8) Hessen, B.; vanderHeijden, H. *J. Am. Chem. Soc.* **1996**, *118*, 11670.
(9) For an example of alkene insertion see: Turculet, L.; Tilley, T. D. *Organometallics* **2004**, *23*, 1542.
(10) For an example of isocyanide and alkene insertion see: Turculet, L.; Tilley, T. D. *Organometallics* **2002**, *21*, 3961.
(11) For an example of alkene insertion see: Jia, L.; Ding, E.; Rheingold, A. L.; Rhatigan, B. *Organometallics* **2000**, *19*, 963.
(12) For examples of heterogeneous/surface catalysts see refs 13−17 and: Dufaud, V. R.; Basset, J. M. *Angew. Chem., Int. Ed.* **1998**, *37*, 806.
(13) Coperet, C.; Chabanas, M.; Saint-Arroman, R. P.; Basset, J. M. *Angew. Chem., Int. Ed.* **2003**, *42*, 156.
(14) Corker, J.; Lefebvre, F.; Lecuyer, C.; Dufaud, V.; Quignard, F.; Choplin, A.; Evans, J.; Basset, J. M. *Science* **1996**, *271*, 966.
(15) Quignard, F.; Choplin, A.; Basset, J. M. *J. Chem. Soc., Chem. Commun.* **1991**, 1589.
(16) Lecuyer, C.; Quignard, F.; Choplin, A.; Olivier, D.; Basset, J. M. *Angew. Chem., Int. Ed.* **1991**, *30*, 1660.
(17) Lefebvre, F.; Thivolle-Cazat, J.; Dufaud, V.; Niccolai, G. P.; Basset, J. M. *Appl. Catal. A: Gen.* **1999**, *182*, 1.
(18) Ghebreab, M. B.; Shalumova, T.; Tanski, J. M.; Waterman, R. *Polyhedron* **2010**, *29*, 42.
(19) Roering, A. J.; Maddox, A. F.; Elrod, L. T.; Chan, S. M.; Ghebreab, M. B.; Donovan, K. L.; Davidson, J. J.; Hughes, R. P.; Shalumova, T.; MacMillan, S. N.; Tanski, J. M.; Waterman, R. *Organometallics* **2009**, *28*, 573.
(20) Waterman, R. *Organometallics* **2007**, *26*, 2492.
(21) Roering, A. J.; Davidson, J. J.; MacMillan, S. N.; Tanski, J. M.; Waterman, R. *Dalton Trans.* **2008**, 4488.
(22) Roering, A. J.; MacMillan, S. N.; Tanski, J. M.; Waterman, R. *Inorg. Chem.* **2007**, *46*, 6855.
(23) Waterman, R. *Dalton Trans.* **2009**, 18.
(24) Sarkar, S.; McGowan, K. P.; Culver, J. A.; Carlson, A. R.; Koller, J.; Peloquin, A. J.; Veige, M. K.; Abboud, K. A.; Veige, A. S. *Inorg. Chem.* **2010**, *49*, 5143.
(25) Golisz, S. R.; Labinger, J. A.; Bercaw, J. E. *Organometallics* **2010**, *29*, 5026.

Published on Web 11/24/2010

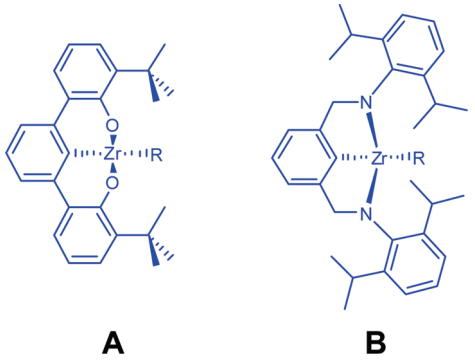

Figure 1. Target molecules: four-coordinate trianionic pincer supported Zr−alkyl species.

coordination, and contribute a maximum of 10 electrons, thus enabling access to coordinatively and electronically unsaturated complexes. Bound to Zr(IV), trianionic pincer ligands leave only one additional site for an anionic ligand. Depending on whether the trianionic pincer ligand is OCO (**A**) or NCN (**B**), the four-coordinate complexes depicted in Figure 1 are potential targets for catalyzing the reactions mentioned above. Not able to adopt a tetrahedral geometry, these complexes will add a substrate to form trigonal-bipyramidal (tbp) or square-pyramidal complexes. As evidence, the pincerate NCN trianionic pincer complexes $[2,6\text{-}^{i}PrNCN]HfX_2^-$ (where X = Cl, Me) are only isolable as salts.[31] If alkenes are the substrates, the insertion can ensue, leading to polyolefin synthesis. However, Bercaw et al. report that bis-phenolate titanium dibenzyl species are not effective precatalysts for propylene polymerization in the absence of an activator.[7] This result prompted an examination into catalyst deactivation and the possibility of isolating or trapping the low-coordinate species **A** and **B** as σ-donor adducts.

This report details the synthesis of $[^{t}BuOCHO]Zr(CH_2Ph)_2$ (**2**) and its subsequent pincer C_{ipso}−H activation by thermolysis or addition of σ-donor ligands. Included are the synthesis and characterization of dimeric zirconium benzyl $\{[^{t}BuOCO]ZrCH_2Ph\}_2$ (**3**), bis-trimethylphosphine zirconium benzyl $[^{t}BuOCO]ZrCH_2Ph(PMe_3)_2$ (**4-PMe$_3$**), bis-tetrahydrofuran zirconium benzyl $[^{t}BuOCO]ZrCH_2Ph(THF)_2$ (**5**), bis-diphenolate zirconium $[^{t}BuOCHO]_2Zr$ (**6**), bis-phenolate pyridyl-pyridine zirconium benzyl $[^{t}BuOCHO]ZrCH_2Ph(\eta^2\text{-}C_5H_4N)py$ (**7**), pyridinyl bis-pyridine zirconium $[^{t}BuOCO]Zr(\eta^2\text{-}C_5H_4N)(py)_2$ (**8**), α-picoline zirconium dibenzyl $[^{t}BuOCHO]Zr(CH_2Ph)_2(\alpha\text{-picoline})$ (**9**), and $[^{t}BuOCHO]Zr(\eta^2(N,C)\text{-6-Me-pyridyl})(\eta^2(N,C\text{-}CH_2)\text{-pyrid-2-yl})$ (**10**).

Results and Discussion

Synthesis and Characterization of $[^{t}BuOCHO]Zr(CH_2Ph)_2$ (2). Alcoholysis between $[^{t}BuOCO]H_3$ (**1**) and 1 equiv of $Zr(CH_2Ph)_4$ in benzene at 23 °C affords $[^{t}BuOCHO]Zr(CH_2Ph)_2$ (**2**) as a pale yellow crystalline solid (eq 1). Attempts to grow single crystals of **2** were unsuccessful, but a combination of ^1H and $^{13}C\{^1H\}$ NMR spectroscopic techniques indicate **2** is a C_s-symmetric dibenzyl complex, with a chelating bis-phenolate ligand. A gHMQC experiment in C_6D_6 reveals a correlation between the pincer C_{ipso}−H proton at 5.17 ppm and a carbon resonance at 113.0 ppm. The $^{13}C\{^1H\}$ NMR spectrum reveals a distinct downfield signal at 159.5 ppm resulting from two equivalent benzyl C_{ipso} agostic interactions with the electronically unsaturated Zr(IV) ion (formally a 12-electron complex without the agostic interaction[33,34]). The ^1H NMR spectrum of **2** indicates the ^{t}Bu groups are also equivalent and their protons resonate at 1.63 ppm. The central ring of the bis-phenolate defines two distinct chemical environments for the methylene protons, appearing at 2.73 and 3.13 ppm. Complex **2** exhibits spectroscopic data and symmetry similar to that of a crystallographically characterized Ti derivative.[7]

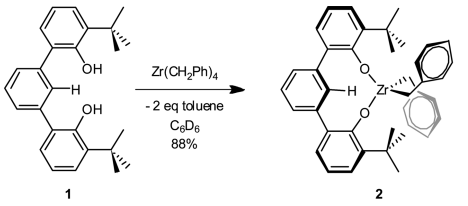

(1)

Synthesis and Characterization of $\{[^{t}BuOCO]ZrCH_2Ph\}_2$ (3). Thermolysis of **2** in benzene for 2 h produces dimeric $\{[^{t}BuOCO]ZrCH_2Ph\}_2$ (**3**) as a yellow microcrystalline solid (eq 2). Slow evaporation of a concentrated ether solution of **3** provides single crystals amenable to X-ray diffraction experiments. Figure 2 depicts the molecular structure of **3** and a truncated fragment that highlights the coordination sphere of the Zr(IV) ion. Table 1 gives crystallographic refinement data. Results from the X-ray diffraction indicate **3** crystallizes in the centrosymmetric monoclinic *I*2/*a* space group and comprises two Zr(IV) ions, two benzyls, and two trianionic OCO pincer ligands. Dimer **3** is C_2-symmetric, and the asymmetric unit consists of half of the dimer. The trianionic pincer ligand binds one Zr ion with an aryloxide linkage and a Zr−C_{ipso} bond, but the second aryloxide bridges to the adjacent zirconium, creating a Zr−Zr distance of 3.4677(8) Å. Zirconium adopts a distorted-trigonal-bipyramidal (tbp) geometry in which C12, C25, and O2#1 occupy the trigonal plane (sum of the angles 359.3(1)°). The axial atoms O1 and O2 are distorted significantly from linearity by ~27° (∠O1−Zr1−O2 = 153.04(9)°).

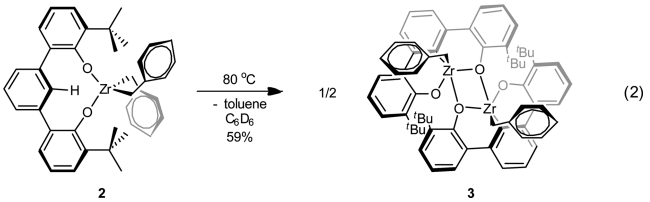

(2)

Reflecting the difference between a η^1-aryloxide and bridging μ_2-aryloxide, the Zr1−O1 bond distance (1.928(2) Å) is considerably shorter than Zr1−O2 (2.185(2) Å) and Zr1−O(2)#1 (2.176(2) Å). Zr−C1(sp^2) (Zr1−C12 = 2.240(3) Å) and

(26) O'Reilly, M.; Falkowski, J. M.; Ramachandran, V.; Pati, M.; Abboud, K. A.; Dalal, N. S.; Gray, T. G.; Veige, A. S. *Inorg. Chem.* **2009**, *48*, 10901.
(27) Korobkov, I.; Gorelsky, S.; Gambarotta, S. *J. Am. Chem. Soc.* **2009**, *131*, 10406.
(28) Sarkar, S.; Carlson, A. R.; Veige, M. K.; Falkowski, J. M.; Abboud, K. A.; Veige, A. S. *J. Am. Chem. Soc.* **2008**, *130*, 1116.
(29) Sarkar, S.; Abboud, K. A.; Veige, A. S. *J. Am. Chem. Soc.* **2008**, *130*, 16128.
(30) Agapie, T.; Day, M. W.; Bercaw, J. E. *Organometallics* **2008**, *27*, 6123.
(31) Koller, J.; Sarkar, S.; Abboud, K. A.; Veige, A. S. *Organometallics* **2007**, *26*, 5438.
(32) Agapie, T.; Bercaw, J. E. *Organometallics* **2007**, *26*, 2957.
(33) Hartwig, J. F. In *Organotransition Metal Chemistry: From Bonding to Catalysis*; University Science Books: Sausalito, CA, 2010; p 64.
(34) Brookhart, M.; Green, M. L. H.; Wong, L. L. *Prog. Inorg. Chem.* **1988**, *36*, 1.

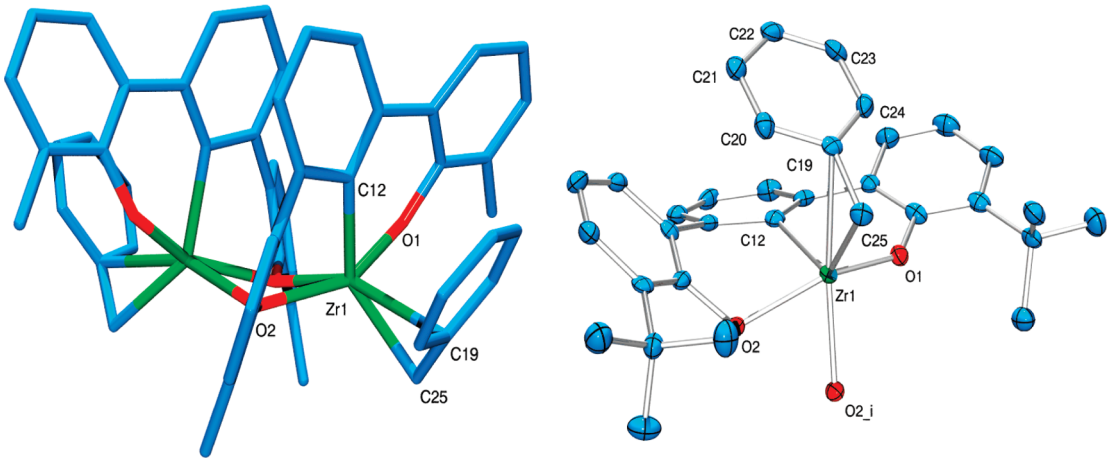

Figure 2. Molecular structure of **3** (left) with ^{t}Bu groups and hydrogen atoms removed for clarity and a truncated drawing of **3** (right) that highlights the Zr coordination sphere with ellipsoids drawn at the 50% probability level. Selected bond distances (Å): Zr1−O1 = 1.928(2), Zr1−O2 = 2.185(2), Zr1−O(2)#1 = 2.176(2), Zr1−C12 = 2.240(3), Zr1−C19 = 2.651(3), Zr1−C25 = 2.277(3), Zr1−Zr1#1 = 3.4677(8). Bond angles (deg): O1−Zr1−O2 = 153.04(9), O1−Zr1−O2#1 = 92.92(9), O1−Zr1−C12 = 83.95(12), O1−Zr1−C25 = 100.72(12), O2−Zr1−O2#1 = 69.61(10), O2−Zr1−C12 = 84.61(11), O2−Zr1−C25 = 106.04(11), O2#1−Zr1−C12 = 113.54(10), O2#1−Zr1−C25 = 123.55(10), C12−Zr1−C25 = 122.18(12).

Table 1. X-ray Crystallographic Structure Parameters and Refinement Data

	3	**4-PMe$_3$**	**6**
empirical formula	$C_{66}H_{68}O_4Zr_2$	$C_{39}H_{52}O_2P_2Zr$	$C_{58}H_{62}O_4Zr$
formula wt	1107.64	705.97	914.3
cryst syst	monoclinic	monoclinic	monoclinic
space group	*I*2/*a*	$P2_1/c$	*C*2/*c*
dimens (mm)	0.33 × 0.25 × 0.05	0.30 × 0.22 × 0.07	0.25 × 0.19 × 0.18
a (Å)	12.9165(17)	11.1851(9)	19.250(2)
b (Å)	26.630(3)	18.2273(15)	15.606(2)
c (Å)	18.979(4)	18.0111(14)	18.149(3)
α (deg)	90	90	90
β (deg)	94.480(3)	101.790(2)	119.316(4)
γ (deg)	90	90	90
V (Å^3)	6508.0(17)	3594.5(5)	4754.0(11)
Z (Å)	4	4	8
abs coeff (mm^{-1})	0.361	0.427	0.278
F(000)	2304	1488	21928
D_{calcd} (g/cm^3)	1.130	1.305	1.277
γ(Mo Kα) (Å)	0.710 73	0.710 73	0.710 73
temp (K)	100(2)	100(2)	100(2)
θ range (deg)	1.53−27.50	1.86−27.50	1.78−27.50
completeness to θ_{max}, %	99.1	99.8	99.9
no. of rflns collected	28 038	31 270	23 052
indep reflections (R_{int})	7430 (0.1350)	8241 (0.0193)	5457 (0.0244)
no. of data/restraints/params	7430/0/331	8241/0/409	5457/0/289
final *R* indices ($I > 2\sigma(I)$)	R1 = 0.0501, wR2 = 0.1033 (4560)	R1 = 0.0227, wR2 = 0.0564 (7474)	R1 = 0.0251, wR2 = 0.0647 (5147)
R indices (all data)	R1 = 0.0862, wR2 = 0.1106	R1 = 0.0263, wR2 = 0.0583	R1 = 0.0271, wR2 = 0.0661
largest diff peak/hole, e/Å^3	0.721/−0.684	0.403/−0.421	0.358/−0.323
goodness of fit on F^2	0.906	1.032	1.064

Zr−C(sp^3) (Zr−C25 = 2.277(3) Å) differ by 0.037(3) Å, indicative of the variation in hybridization at each carbon. The benzyl forms an agostic interaction by coordination between C19$_{ipso}$ and the zirconium (Zr1−C19 = 2.651(3) Å). The Zr−C$_{ipso}$ agostic interaction is comparable to that in other electronically unsaturated monobenzyl complexes, such as 2.648(2) Å for CH[(CH$_3$)$_2$SiNAr]$_3$ZrCH$_2$Ph (where Ar = *p*-fluorophenyl, **I**), and 2.753(7) and 2.795(8) Å for CH[(CH$_3$)$_2$-SiNAr′]$_3$ZrCH$_2$Ph (where Ar′ = *p*-tolyl, **II**; two crystallographically independent molecules).[6] Similar Zr−C−C$_{ipso}$ bond angles are found for this set of monobenzyl complexes (**3**, 87.31(1)°; **I**, 88.24(14)°; **II**, 91.4(5) and 93.1(5)°), though in **II** the angle is larger to complement the slightly weaker agostic bond.[6] The related complex Zr(OAr)(CH$_2$Ph)$_3$ (OAr = 2,6-di-*tert*-butylphenoxide) exhibits a much stronger agostic interaction, and the angle, 84°, is more acute.[35] According to Tonks and Bercaw et al., when the metal ion is electronically unsaturated the ligand will distort to maximize pπ−dπ donation from the aryloxides.[36] Formally a 12-electron complex without aryloxide pπ−dπ donation, the OCO ligand distorts, evidenced by the twisted central ring of the terphenyl frame. The central rings twist by ∼28 and ∼46° relative to the two outer ring planes of the pincer. The severe 46° distortion occurs because that ring contains the bridging alkoxide. An isostructural Ti derivative exhibits similar distortions.[25]

(35) Latesky, S. L.; Mcmullen, A. K.; Niccolai, G. P.; Rothwell, I. P.; Huffman, J. C. *Organometallics* **1985**, *4*, 902.
(36) Tonks, I. A.; Henling, L. M.; Day, M. W.; Bercaw, J. E. *Inorg. Chem.* **2009**, *48*, 5096.

The ^{1}H and ^{13}C{^{1}H} NMR spectra of **3** are consistent with the solid-state observations. The benzyl methylene protons are diastereotopic (J = 10 Hz) and resonate as two doublets at 2.57 and 2.87 ppm. The corresponding carbon resonates slightly downfield compared with that in **2** (65.5 and 66.5 ppm) at 67.0 ppm. Reflecting the different binding modes of the alkoxides, two resonances appear for the ^{t}Bu proton at 1.23 and 1.78 ppm. The pincer Zr−C_{ipso} appears well downfield at 190.9 ppm, easily distinguishable from the unactivated bisphenolate form in **2** (113.0 ppm).

Synthesis and Characterization of [^{t}BuOCO]ZrCH$_2$Ph(PMe$_3$)$_2$ (4-PMe$_3$), [^{t}BuOCO]ZrCH$_2$Ph(THF)$_2$ (5), and [^{t}BuOCHO]$_2$Zr (6). Thermolysis of **2** leads to the formation of dimer **3**. The ^{t}Bu groups on the OCO ligand are not sufficiently bulky to prevent dimerization, since they adopt bridging positions between the two Zr ions. Stabilizing mononuclear alkyl species is possible by addition of PMe_3. Treating **2** with 2 equiv of PMe_3 yields the bis-trimethylphopshine adduct [^{t}BuOCO]ZrCH$_2$Ph(PMe$_3$)$_2$ (**4-PMe$_3$**) as yellow crystalline blocks upon precipitation from benzene (eq 3). Once precipitated, the complex does not redissolve and is insoluble in common solvents, including the halogenated solvents dichloromethane and chloroform. The reaction mixture was amenable to multinuclear (^{1}H, ^{13}C{^{1}H}, and ^{31}P{^{1}H}) NMR experiments prior to precipitation.

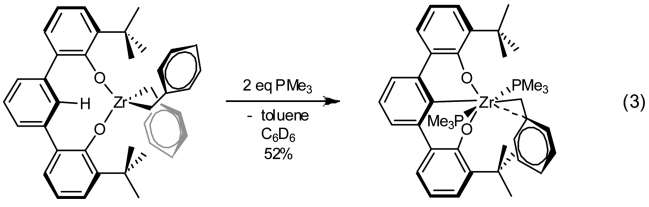

(3)

The ^{1}H NMR spectrum of **4-PMe$_3$** in C_6D_6 reveals symmetric ^{t}Bu groups with protons that resonate at 1.67 ppm. In the ^{13}C{^{1}H} spectrum, the corresponding ^{t}Bu carbons appear at 30.8 and 35.7 ppm. The chemically equivalent benzyl methylene protons appear as a singlet at 2.77 ppm, whereas in complex **3** the protons are diastereotopic. Resonating upfield from free PMe_3 (0.86 ppm), the equivalent PMe_3 protons appear at 0.33 ppm. The PMe_3 methyl carbons couple to phosphorus as a pseudotriplet as a consequence of virtual coupling at 13.0 ppm (J_{PC} = 13 Hz).[37−39] The ^{31}P{^{1}H} NMR spectrum of **4-PMe$_3$** exhibits a single resonance at 31.5 ppm.

The yellow blocks that deposit from the reaction medium are single crystals, and an X-ray diffraction experiment provides the solid-state structure of **4-PMe$_3$**. Figure 3 depicts the monomeric molecular structure of **4-PMe$_3$**, which comprises one trianionic pincer, two PMe_3 ligands, and one benzyl. Table 1 gives refinement data. Including the agostic interaction, the coordination geometry of **4-PMe$_3$** is best described as a distorted monocapped octahedron. The trans-PMe_3 ligands are bent toward the pincer ligand by 20° (∠P1−Zr1−P2 = 159.611(11)°), and the Zr−P bond lengths differ slightly (Zr1−P1 = 2.8108(4)

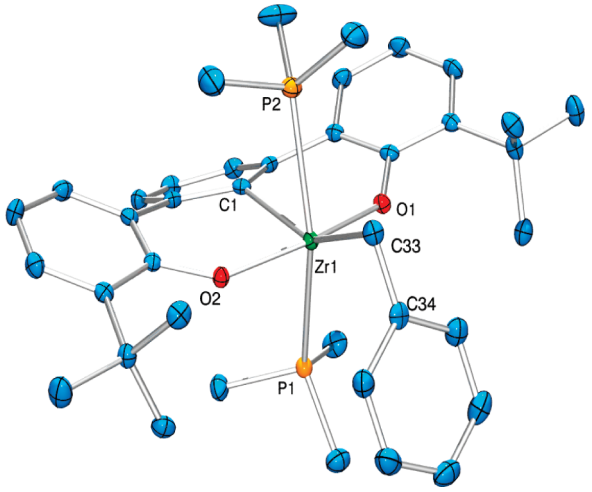

Figure 3. Molecular structure of **4-PMe$_3$** with ellipsoids drawn at the 50% probability level and hydrogen atoms removed for clarity. Selected bond distances (Å): Zr1−O1 = 2.0032(9), Zr1−O2 = 2.0063(9), Zr1−C1 = 2.3065(12), Zr1−C33 = 2.3330(13), Zr1−C34 = 2.7976(13), Zr1−P1 = 2.8108(4), Zr1−P2 = 2.7696(4). Bond angles [(deg): O1−Zr1−O2 = 164.32(4), O1−Zr1−C1 = 83.65(4), O1−Zr1−P1 = 86.48(3), O1−Zr1−P1 = 89.07(3), O1−Zr1−C33 = 98.63(4), O2−Zr1−P1 = 86.03(3), O2−Zr1−P2 = 93.18(3), O2−Zr1−C1 = 82.01(4), O2−Zr1−C33 = 96.96(4), C1−Zr1−P1 = 85.19(3), C1−Zr1−P2 = 74.54(3), C1−Zr1−C33 = 149.79(5), C33−Zr1−P1 = 124.96(3), C33−Zr1−P2 = 75.38(3), P1−Zr1−P2 = 159.6(1).

and Zr1−P2 = 2.7696(4) Å). These bond lengths are somewhat longer than typically observed for Zr−phosphine complexes.[40−46] Short bonds appear in the complexes [Cp$_2$Zr(Et)(PMe$_3$)]$^+$ (Zr−P = 2.691(4) Å),[47] Cp$_2$Zr(cyclohexyne)PMe$_3$ (Zr−P = 2.689(3) Å),[48] and [Cp$_2$Zr(benzdiyne)PMe$_3$]$_2$ (Zr−P = 2.667(2) Å).[49] In contrast, Cp$_2$Zr(CH$_2$CH$_2$B(C$_6$F$_5$)$_3$)(PPh$_2$Me) features a longer bond due to the larger diphenylmethylphosphine ligand (Zr−P = 2.828(1) Å).[50]

Another distortion appears for the benzyl ligand, which is bent toward one of the PMe_3 ligands by 30° to accommodate an agostic interaction (∠C1−Zr1−C33 = 149.79(5)°). Interestingly, C34$_{ipso}$ of the benzyl is nearly linearly aligned with the C1 carbon of the pincer, creating the angle ∠C1−Zr1−C34 = 178.10(4)°. The agostic interaction is weaker in **4-PMe$_3$** (Zr1−C34$_{ipso}$ = 2.7976(13) Å) than in **3** (Zr1−C19$_{ipso}$ = 2.651(3) Å), but a correspondingly shorter trans Zr1−C1$_{pincer}$ bond in **4-PMe$_3$** is not observed. Instead, the Zr1−C1$_{pincer}$ bond is longer in **4-PMe$_3$** (Zr1−C1 = 2.3065(12) Å) than in **3** (Zr1−C12 = 2.240(3) Å). More impressive is the acute 74.54(3)° angle between P2 and C1 on the pincer ligand, which must be forced

(37) For a discussion of virtual coupling see ref 38 and: Drago, R. S. In *Physical Methods in Chemistry*; Saunders: Philadelphia, 1977; p 222.
(38) Jordan, R. F.; Bajgur, C. S.; Dasher, W. E.; Rheingold, A. L. *Organometallics* **1987**, *6*, 1041.
(39) Mann, B. E.; Shaw, B. L.; Stainban, Re *J. Chem. Soc., Chem. Commun.* **1972**, 151.
(40) Basta, R.; Harvey, B. G.; Arif, A. M.; Ernst, R. D. *Inorg. Chim. Acta* **2004**, *357*, 3883.
(41) Pikies, J.; Baum, E.; Matern, E.; Chojnacki, J.; Grubba, R.; Robaszkiewicz, A. *Chem. Commun.* **2004**, 2478.
(42) Ramakrishna, T. V. V.; Lushnikova, S.; Sharp, P. R. *Organometallics* **2002**, *21*, 5685.
(43) Lee, H.; Desrosiers, P. J.; Guzei, I.; Rheingold, A. L.; Parkin, G. *J. Am. Chem. Soc.* **1998**, *120*, 3255.
(44) Procopio, L. J.; Carroll, P. J.; Berry, D. H. *J. Am. Chem. Soc.* **1991**, *113*, 1870.
(45) Vandenhende, J. R.; Hessen, B.; Meetsma, A.; Teuben, J. H. *Organometallics* **1990**, *9*, 537.
(46) Cotton, F. A.; Diebold, M. P.; Kibala, P. A. *Inorg. Chem.* **1988**, *27*, 799.
(47) Jordan, R. F.; Bradley, P. K.; Baenziger, N. C.; Lapointe, R. E. *J. Am. Chem. Soc.* **1990**, *112*, 1289.
(48) Buchwald, S. L.; Lum, R. T.; Dewan, J. C. *J. Am. Chem. Soc.* **1986**, *108*, 7441.
(49) Buchwald, S. L.; Lucas, E. A.; Dewan, J. C. *J. Am. Chem. Soc.* **1987**, *109*, 4396.
(50) Sun, Y. M.; Piers, W. E.; Rettig, S. J. *Chem. Commun.* **1998**, 127.

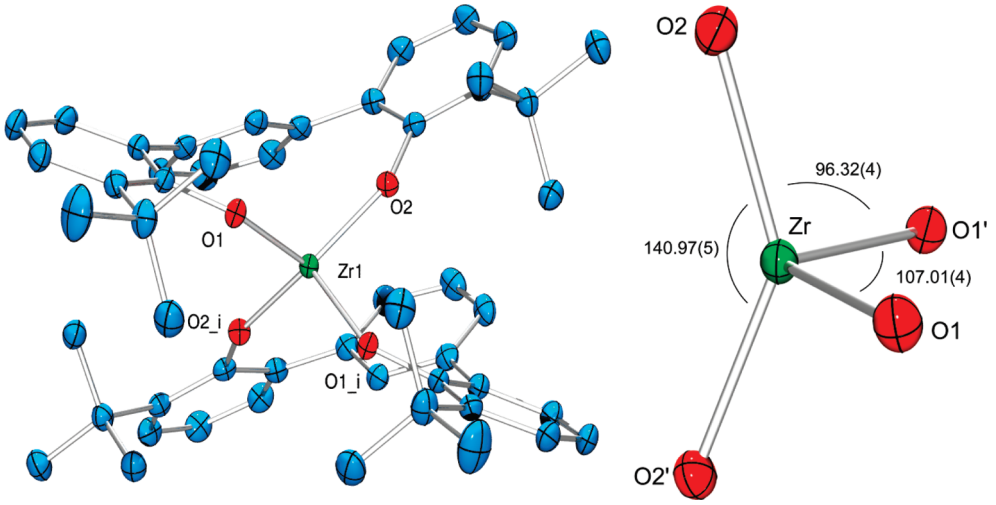

Figure 4. Molecular structure of **6** (left) with ellipsoids drawn at the 50% probability level and hydrogen atoms and the solvent of crystallization molecule (benzene) removed for clarity and the truncated structure of **6** (right) highlighting the Zr(IV) coordination sphere. Selected bond distances (Å): Zr1−O1 = 1.9733(9), Zr1−O2 = 1.9835(9), Zr1−C12 = 2.8162(13). Bond angles (deg): O1−Zr1−O1#1 = 105.89(5), O1−Zr1−O2 = 107.01(4), O1−Zr1−O2#1 = 96.32(4), O1#1−Zr1−O2 = 96.32(4), O1#1−Zr1−O2#1 = 107.01(4), O2−Zr1−O2#1 = 140.97(5).

into this position by the benzyl ligand; the P1−Zr−C1 angle is larger (85.19(3)°). Addition of 1 equiv of PPh_3 to **2** in C_6D_6 does not produce the corresponding mono- or bis-PPh_3 complex. Instead, no reaction occurs at 23 °C, and refluxing the solution results in formation of dimer **3**.

Inducing the pincer C_{ipso}-H bond activation by addition of a σ-donor ligand provides compelling evidence for a general approach to installing the trianionic form of the pincer ligand. For example, treating **2** with 2 equiv of THF in C_6D_6 results in the bis-THF adduct [^{t}BuOCO]ZrCH_2Ph$(THF)_2$ (**5**; eq 4). An alternative synthesis of compound **5** is possible by stirring an equimolar ratio of **1** and Zr$(CH_2Ph)_4$ at 23 °C in THF.

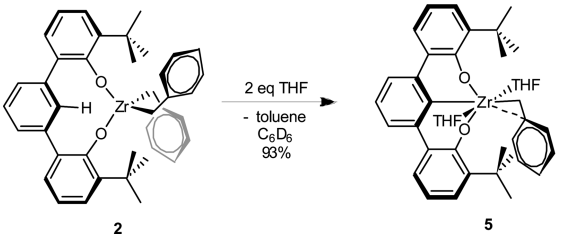

(4)

^{1}H and ^{13}C{^{1}H} NMR spectroscopy and combustion analysis confirm the composition and purity of **5**. The ^{1}H NMR spectrum of **5** exhibits two broad resonances at 0.96 and 3.48 ppm that integrate to eight protons each and are attributable to the THF ligands. In comparison with free THF (1.40 and 3.57 ppm), the coordinated THF protons are shifted upfield.[51,52] In the ^{13}C{^{1}H} spectrum, the corresponding THF carbon resonances appear at 25.4 and 72.3 ppm. Characteristic benzyl protons resonate at 2.89 ppm, and the corresponding methylene ^{13}C resonance appears at 58.8 ppm. The 18 protons of the ^{t}Bu resonate as a singlet at 1.76 ppm, and the corresponding quaternary and primary carbons appear at 31.1and 35.7 ppm, respectively. A singlet at 189.9 ppm is typical for the pincer carbon bound to Zr and compares favorably with **3** (190.9 ppm) and **4-PMe$_3$** (194.5 ppm). The additional 14 aromatic protons resonate between 6.46 and 7.70 ppm, and the corresponding carbons are located between 119.8 and 157.6 ppm.

Spatially cumbersome σ-donor ligands such as PPh_3 do not promote the aryl C−H bond activation. Treating **2** with 2 equiv of the smaller PMe_2Ph, however, results in the formation of the mono-PMe_2Ph complex [^{t}BuOCO]ZrCH_2Ph(PMe_2Ph_2) (**4-PMe$_2$Ph**; see the Supporting Information). Attempts to recrystallize and purify **4-PMe$_2$Ph** lead to precipitation of a minor amount of the bis-diphenolate complex [^{t}BuOCHO]$_2$Zr (**6**). Only present as a minor product, an alternative synthesis that provides analytically pure **6** in 68% yield involves adding 2 equiv of **1** directly to Zr$(CH_2Ph)_4$ in benzene (eq 5). [^{t}BuOCHO]$_2$Zr (**6**) is insoluble in hydrocarbon, ethereal, and halogenated solvents; moreover, DMF and DMSO do not dissolve **6**.

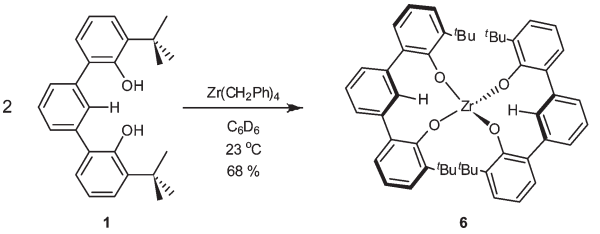

(5)

As **6** was not amenable to solution-phase characterization, its molecular structure was determined by subjecting single crystals that deposit from the reaction medium to an X-ray diffraction experiment. Figure 4 depicts the molecular structure of **6**, the figure caption contains pertinent bond lengths and angles, and Table 1 gives crystal refinement data. Two diphenolate ligands bond to one Zr(IV) ion, rendering the complex C_2 symmetric. The zirconium ion sits on a 2-fold rotation axis, and the asymmetric unit comprises half of the complex and a half-molecule of solvent (benzene). Within the asymmetric unit, the two Zr−O distances differ slightly (Zr1−O1 = 1.9733(9) Å and Zr1−O2 = 1.9835(9) Å). One large angle between opposing ligand alkoxides imparts

(51) Fulmer, G. R.; Miller, A. J. M.; Sherden, N. H.; Gottlieb, H. E.; Nudelman, A.; Stoltz, B. M.; Bercaw, J. E.; Goldberg, K. I. *Organometallics* **2010**, *29*, 2176.

(52) Gottlieb, H. E.; Kotlyar, V.; Nudelman, A. *J. Org. Chem.* **1997**, *62*, 7512.

Scheme 1. Synthetic Details for the Synthesis of [^{t}BuOCHO]Zr(CH$_2$Ph)(η-C$_5$H$_4$N)py (7) and [^{t}BuOCO]Zr(η-C$_5$H$_4$N)(py)$_2$ (8)

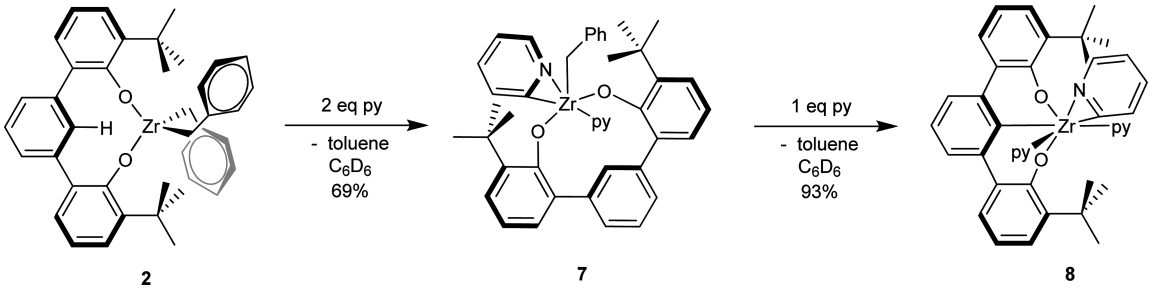

a quasi-sawhorse geometry to the complex ($\angle$O2−Zr1−O2#1 = 140.97(5)°; see the right-hand side of Figure 4). As a consequence of having to span the terphenyl framework, the angle between alkoxides within one diphenolate splays to $\angle$O1−Zr1−O2 = 107.01(4)°. The most notable feature of complex **6** is that the two diphenolates are oriented face to face but are rotated such that one pincer central ring π-stacks with a pincer external ring of the opposite ligand. This subtle twist allows one of the ^{t}Bu groups to slip in between two ^{t}Bu groups from the opposite diphenolate.

Synthesis and Characterization of [^{t}BuOCHO]Zr(CH$_2$Ph)(η-C$_5$H$_4$N)py (7) and [^{t}BuOCO]Zr(η-C$_5$H$_4$N)(py)$_2$ (8). Treatment of **2** with 2 equiv of pyridine (py) leads to the formation of [^{t}BuOCHO]Zr(CH$_2$Ph)(η-C$_5$H$_4$N)py (**7**). Unlike the case when PMe$_3$ and THF add to **2**, the bis-py adduct [^{t}BuOCO]-Zr(CH$_2$Ph)py$_2$ is not isolable; instead, immediate activation of the *o*-C−H bond on one py occurs, with concomitant liberation of toluene (Scheme 1). Pentamethylcyclopentadienyl (Cp*) zirconium alkyl cationic complexes exhibit similar pyridine *o*-CH metalation.[53−61] Complex **7** is not stable in solution at ambient temperature; however, the reaction end point can be determined by monitoring the reaction periodically by ^{1}H NMR spectroscopy. Typically the reaction takes 2 h to complete. Removal of all volatiles and washing the residual solid with pentane provides **7** as a crystalline yellow powder in 69% yield. Once isolated in the solid state, complex **7** is stable, but redissolving **7** for the purpose of spectroscopic analysis results in further reactivity. Fortunately, single crystals amenable to an X-ray diffraction study provide the molecular structure of **7**. Figure 5 depicts the results of the structural refinement as well as pertinent bond lengths and angles, and Table 2 gives refinement data.

Complex **7** comprises one chelating dianionic bis-phenolate ligand, one benzyl group, one pyridine, and one ortho-metalated pyridine. The Zr(IV) ion adopts a square-pyramidal coordination environment. The diphenolate aryloxides bind trans to each other in the basal plane, the *N*-bound pyridine and ortho-metalated pyridine occupy the remaining basal sites, and the benzyl sits in the apical position. In contrast to **3** and **4-PMe$_3$**, no agostic interaction forms between the Zr(IV) ion and the benzyl C$_{ipso}$ atom; the Zr1−C12 distance is 2.862(3) Å. In fact, the benzyl arene ring leans toward one side of the molecule (O2), causing one of the Zr−O bonds to elongate; the experimental values are Zr1−O1 = 1.988(2) Å and Zr1−O2 = 2.012(2) Å. In the solid state, the N-bound pyridine twists relative to the ortho-metalated ring by ~88°. The Zr1−N1 and Zr1−N2 bond distances vary significantly by 0.201(2) Å, reflecting the different binding modes (η^1 vs η^2). Interestingly, the η-pyridinyl group orients in two distinct ways by situating the N atom exo (0.75(2) site occupancy) versus endo (0.25(2) site occupancy) relative to the apical benzyl. In solution, the η-pyridinyl isomerizes between the two positions faster than the ^{1}H NMR time scale, thus exhibiting only one set of resonances (vide infra).

An appropriately shorter Zr−C bond results for the ortho-metalated pyridine (Zr1−C39 = 2.254(2) Å) versus the Zr−benzyl bond (Zr1−C27 = 2.327(3) Å). C$_{ipso}$ of the central ring in the diphenolate ligand is aligned with the Zr−CH$_2$ axis with an angle of $\angle$C12−Zr1−C27 = 154.07(3)°, but it is unreasonably distant (Zr−C12 = 2.862(3) Å) to form a strong interaction. Instead, C$_{ipso}$ most likely resides in that position naturally due to the chelate.

Analytically pure **7** will precipitate from C$_6$D$_6$ upon its formation, but forcing **7** to redissolve with heat promotes subsequent reactivity (~17% conversion to compound **8**, Scheme 1). To circumvent these problems, it is necessary to complete ^{1}H NMR and ^{13}C{^{1}H} NMR spectroscopic analysis on **7** generated in situ, prior to complete deposition. The ^{1}H NMR spectrum of **7** reveals a broad singlet at 2.79 ppm for the benzyl CH$_2$ protons and a singlet at 1.30 ppm for the ^{t}Bu protons. For the benzyl CH$_2$ protons to be equivalent, it must invert and rotate freely in solution. Broad resonances attributable to the η^1-pyridine ligand appear at 9.30, 8.83, and 7.61 ppm. In the ^{13}C{^{1}H} NMR spectrum of **7** a resonance appears at 201.1 ppm, attributable to the Zr−C$_{pyridinyl}$ carbon.[57,59−61] Other resonances consistent with the solid-state structure include a benzyl CH$_2$ at 57.8 ppm and *C*(CH$_3$)$_3$ and C(*C*H$_3$)$_3$ resonances at 35.5 and 30.4 ppm, respectively.

With an extra 1 equiv of pyridine present, complex **7** converts to the trianionic pincer complex [^{t}BuOCO]Zr(η-C$_5$H$_4$N)(py)$_2$ (**8**) in 93% yield (Scheme 1). A suite of NMR spectroscopic techniques permits the identification of complex **8**. Obtained at −60 °C in toluene-d_8, the ^{1}H−^{1}H and ^{1}H−^{13}C (one-bond and long-range) couplings within the DQCOSY, gHMQC, and gHMBC spectra permit the absolute assignment of each ^{1}H and ^{13}C{^{1}H} NMR resonance (see Table S1 in the Supporting Information for the complete assignment). At 25 °C, the pyridines self-exchange and as a consequence exhibit broad

(53) For examples of Zr−pyridinyl and Zr−pyridyl complexes see refs 54−61 and: Jordan, R. F.; Taylor, D. F.; Baenziger, N. C. *Organometallics* **1990**, *9*, 1546.
(54) Guram, A. S.; Swenson, D. C.; Jordan, R. F. *J. Am. Chem. Soc.* **1992**, *114*, 8991.
(55) Guram, A. S.; Jordan, R. F.; Taylor, D. F. *J. Am. Chem. Soc.* **1991**, *113*, 1833.
(56) Guram, A. S.; Jordan, R. F. *Organometallics* **1991**, *10*, 3470.
(57) Jordan, R. F.; Guram, A. S. *Organometallics* **1990**, *9*, 2116.
(58) Jordan, R. F.; Taylor, D. F. *J. Am. Chem. Soc.* **1989**, *111*, 778.
(59) Oishi, M.; Kato, T.; Nakagawa, M.; Suzuki, H. *Organometallics* **2008**, *27*, 6046.
(60) Krut'ko, D. P.; Kirsanov, R. S.; Belov, S. A.; Borzov, M. V.; Churakov, A. V.; Howard, J. A. K. *Polyhedron* **2007**, *26*, 2864.
(61) Bradley, C. A.; Lobkovsky, E.; Chirik, P. J. *J. Am. Chem. Soc.* **2003**, *125*, 8110.

resonances at 8.73 (*o*-CH, 4H), 6.20 (*m*-CH), and 6.60 ppm (*p*-CH). Figure 6 depicts the results of a variable-temperature ^{1}H NMR study from −60 to 50 °C in toluene-d_8. Line-shape analysis provides the activation energy of $\Delta G^{\ddagger}$(298 K) = 12.0(3) kcal/mol for the self-exchange ($\Delta S^{\ddagger}$ = −5.5(6) cal/(mol K), $\Delta H^{\ddagger}$ = 10.4(1) kcal/mol). At −60 °C, the exchange process slows and the resonances at 8.73 and 6.20 ppm split into two at 9.01 and 8.64 ppm and at 6.40 and 6.31 ppm, respectively. The resonance at 6.60 ppm sharpens as the temperature decreases but does not resolve into two signals. Rapid exchange between the pyridines, even at −60 °C, prevents assignment of cis versus trans pyridines. Though the pyridines self-exchange, they do not exchange with the η-pyridinyl, even at 55 °C. The ^{15}N NMR spectrum of **8** at −60 °C reveals three resonances at 290.1 (η-pyridinyl), 280.0 (py), and 278.3 ppm (py). Important ^{13}C{^{1}H} NMR assignments include the Zr−C_{pincer} carbon at 188.0 ppm and the Zr−$C_{pyridinyl}$ carbon at 207.2 ppm, which is downfield from **7** but is within the range for other reported Zr−pyridinyls.[57,59−61]

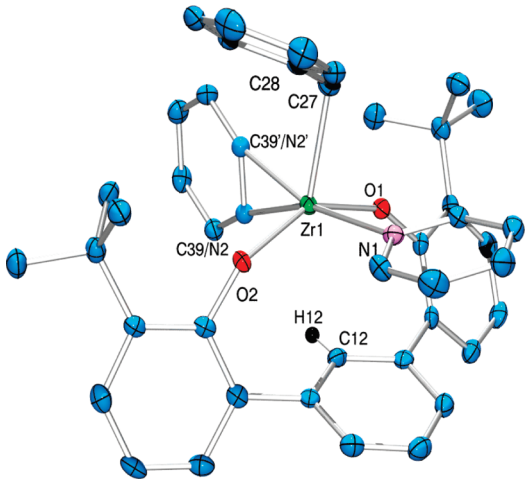

Figure 5. Molecular structure of **7** with ellipsoids drawn at the 50% probability level and hydrogen atoms removed for clarity. Selected bond distances (Å): Zr1−O1 = 1.988(2), Zr1−O2 = 2.012(2), Zr1−N1 = 2.403(2), Zr1−N2 = 2.202(2), Zr1−C27 = 2.327(3), Zr1−C39 = 2.254(2), Zr1−C12 = 2.863(0), Zr1−C28 = 3.230(0). Bond angles (deg): O1−Zr1−O2 = 148.64(7), O1−Zr1−N1 = 83.72(7), O1−Zr1−N2 = 98.50(7), O1−Zr1−C27 = 97.52(9), O1−Zr1−C39 = 87.87(8), O2−Zr1−N1 = 87.82(7), O2−Zr1−N2 = 98.20(7), O2−Zr1−C27 = 110.54(9), O2−Zr1−C39 = 90.92(8), N2−Zr1−N1 = 163.25(8), N2−Zr1−C27 = 83.77(10), N2−Zr1−C39 = 34.77(8), C27−Zr1−N1 = 79.48(9), C39−Zr1−N1 = 161.54(8), C39−Zr1−C27 = 118.02(10).

Synthesis and Characterization of [^{t}BuOCHO]Zr(CH_2Ph)$_2$-(α-picoline) (9) and [^{t}BuOCHO]Zr(η^2(*N,C*)-6-Me-pyridyl)(η^2-(*N,C*-CH_2)-pyrid-2-yl) (10). Addition of THF, PMe_3, or py to **2** induces rapid toluene elimination and aromatic C−H bond activation. Coordination of the substrate must initiate the C−H bond activation, because no reaction occurs upon addition of 2,6-lutidine. In contrast, α-picoline easily binds upon the addition of 2 equiv. Adduct **9** forms prior to any C−H bond activation or toluene elimination event (Scheme 2), providing insight into the mechanism. Yellow blocks of [^{t}BuOCHO]Zr-(CH_2Ph)$_2$(α-picoline) (**9**; 88%), which are single crystals, deposit as the reaction mixture is slowly warmed to ambient temperature.

An X-ray diffraction experiment provides satisfactory data to solve the molecular structure of **9**. Figure 7 depicts the molecular structure of **9**, the figure caption gives pertinent bond lengths and angles, and Table 2 gives refinement data. The structural refinement indicates that the asymmetric unit contains **9** and two benzene solvent molecules. The Zr(IV) ion adopts a C_1-symmetric square-pyramidal geometry in which one benzyl, the α-picoline, and the diphenolate comprise the basal plane. The second benzyl group occupies the apical position, and its phenyl ring leans to one side of the complex. The most striking feature is that the α-picoline resides in two sites with occupancy factors refined at 0.738(4) for the major isomer and 0.264(4) for the minor isomer. A consequence of the apical benzyl lean and sterics,

Table 2. X-ray Crystallographic Structure Parameters and Refinement Data

	7	9	10
empirical formula	$C_{90}H_{90}N_4O_4Zr_2$	$C_{55}H_{58}NO_2Zr$	$C_{38}H_{40}N_2O_2Zr$
formula wt	1474.10	856.24	647.94
cryst syst	monoclinic	triclinic	monoclinic
space group	$C2/c$	$P\bar{1}$	$P2_1/c$
dimens (mm)	0.16 × 0.13 × 0.03	0.14 × 0.07 × 0.04	0.12 × 0.11 × 0.04
a (Å)	29.1174(9)	12.1545(7)	11.4471(10)
b (Å)	16.0255(5)	14.6482(9)	17.0000(15)
c (Å)	19.8750(6)	14.7222(9)	16.9534(14)
α (deg)	90	63.211(3)	90
β (deg)	118.469(1)	74.803(3)	97.364(5)
γ (deg)	90	84.545(4)	90
V (Å^3)	8152.6(4)	2257.2(2)	3271.9(5)
Z (Å)	4	2	4
abs coeff (mm^{-1})	0.306	2.309	0.371
F(000)	3080	902	1352
D_{calcd} (g/cm^3)	1.201	1.260	1.315
γ(Mo Kα) (Å)	0.71073	1.54178	0.71073
temp (K)	100(2)	100(2)	100(2)
θ range (deg)	1.59−27.50	3.38−66.18	1.70−27.50
completeness to θ_{max} (%)	100.0	96.2	100.0
no. of rflns collected	40 404	40 219	46 655
no. of indep rflns (R_{int})	9356 (0.0652)	7611 (0.0720)	7507 (0.0844)
no. of data/restraints/params	9356/0/447	7611/0/530	7507/0/407
final R indices ($I > 2\sigma(I)$)	R1 = 0.0456, wR2 = 0.1032 (6583)	R1 = 0.0325, wR2 = 0.0763 (6494)	R1 = 0.0365, wR2 = 0.0701 (5084)
R indices (all data)	R1 = 0.0719, wR2 = 0.1095	R1 = 0.0410, wR2 = 0.0799	R1 = 0.0680, wR2 = 0.0769
largest diff peak/hole (e Å^3)	0.478/−0.304	0.882/−0.627	0.425/−0.421
goodness of fit on F^2	1.114	0.985	0.914

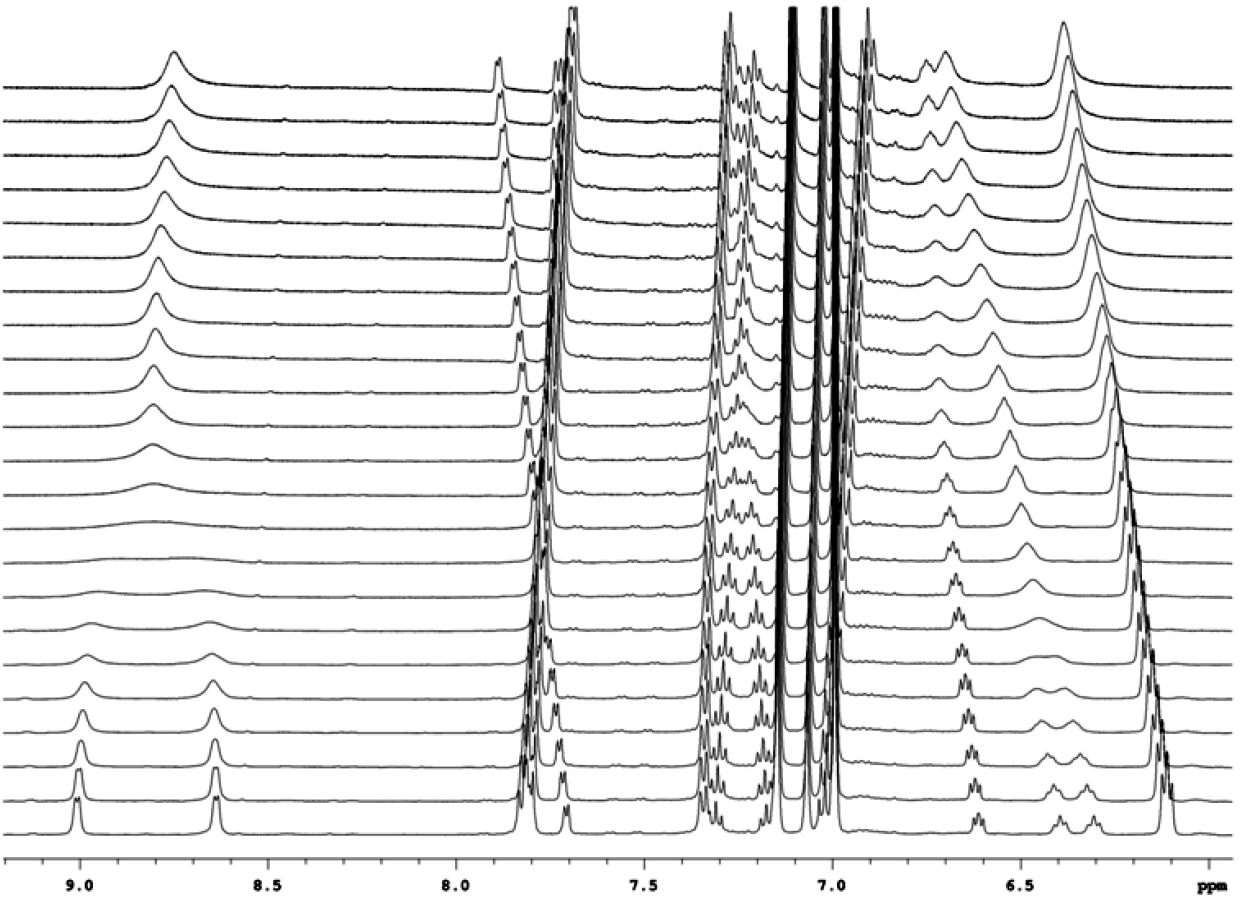

Figure 6. Stacked spectra from a variable-temperature ^{1}H NMR experiment of [^{t}BuOCO]Zr(η-C_5H_4N)(py)$_2$ (**8**) in toluene-d_8 from −60 to 50 °C.

Scheme 2. Synthetic Details for the Synthesis of [^{t}BuOCHO]Zr(CH_2Ph)$_2$(α-picoline) (9) and [^{t}BuOCHO]Zr(η^2(*N,C*)-6-Me-pyridyl)-(η^2(*N,C*-CH_2)-pyrid-2-yl) (10)

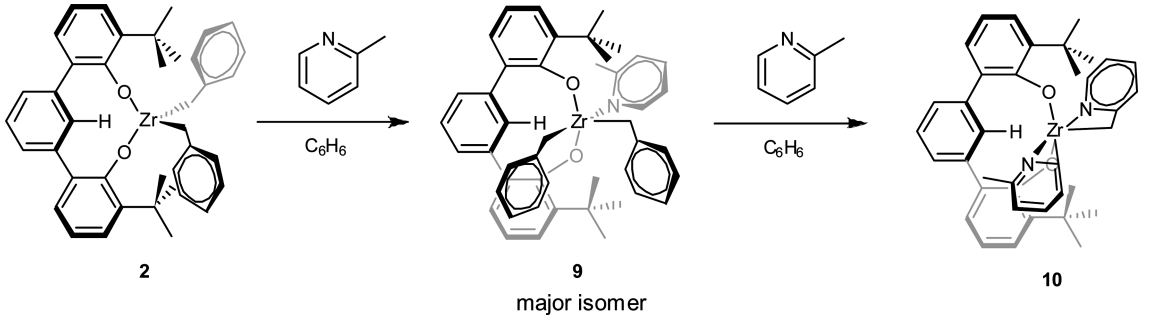

the major isomer places the methyl group of the α-picoline on the opposite side. The two benzyl ligands are cis (∠C27−Zr1−C34 = 88.33(9)°), and the angle at the benzyl methylenes differ, with the more acute angle providing a slightly longer Zr−C bond (∠Zr1−C27−C28 = 98.82(1)° corresponds to Zr−C27 = 2.302(2) Å and ∠Zr1−C34−C35 = 116.45(0)° corresponds to 2.289(2) Å).

Complex **9** is insoluble in hydrocarbon solvents but will dissolve in chlorinated solvents. Once in solution, subsequent reactivity ensues (vide infra). In fact, the 2 equiv of α-picoline used in the synthesis are necessary to promote the exclusive formation of **9**; otherwise, a mixture of products forms. Conducting the NMR experiments at −25 °C slows the reactivity and provides sufficient time to complete the solution-phase spectroscopic characterization (an unavoidable 5% of complex **10** forms). Complementary to the solid state α-picoline disorder, resonances attributable to the two isomers appear in the ^{1}H NMR spectrum, though some are indistinguishable due to overlap. Distinct resonances for the isomers include two sets of benzyl methylenes at 1.83 and 2.56 ppm (major) and at 2.63 and 2.73 ppm (minor) in a 6.7:1 ratio. The corresponding $^{13}C\{^1H\}$ resonances for the benzyl methylenes appear at 68.1 and 68.9 ppm, but the minor isomer resonances are undetectable due to the lower concentration. Both isomer ^{t}Bu protons must overlap, as only a single resonance appears at 1.75 ppm. The observation of one ^{t}Bu resonance also indicates the complex is C_s symmetric in solution, implying fast rotation around the Zr−benzyl bonds. A broad resonance integrating to three protons appears at 2.19 ppm, which is shifted from free α-picoline (2.38 ppm). Dramatically

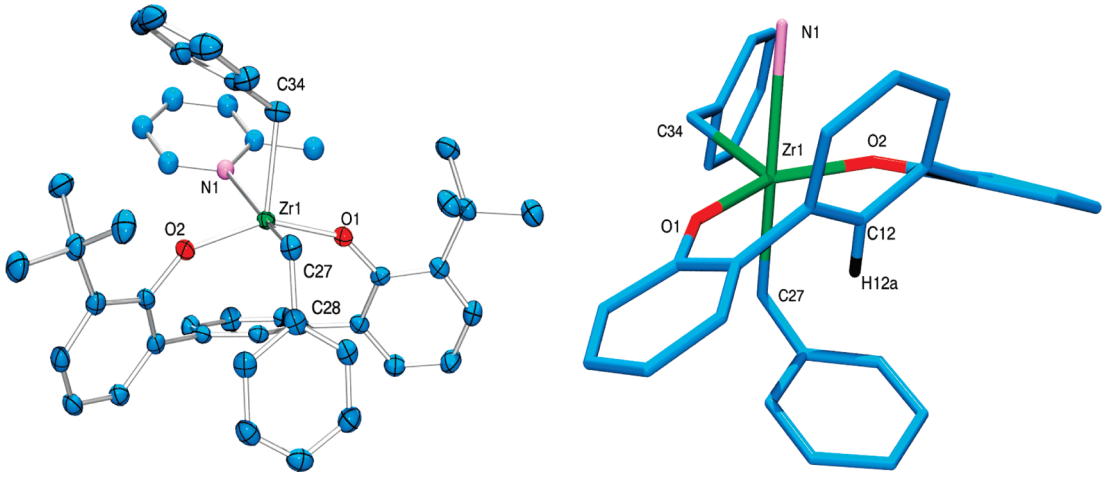

Figure 7. Molecular structure of **9** (left) with ellipsoids drawn at the 50% probability level and hydrogen atoms removed for clarity and the truncated structure of **9** (right) highlighting the Zr(IV) coordination sphere. Selected bond distances (Å): Zr1−O1 = 1.9759(16), Zr1−O2 = 1.9987(15), Zr1−N1 = 2.4941(13), Zr1−N1′ = 2.525(4), Zr1−C27 = 2.302(2), Zr1−C34 = 2.289(2), Zr1−C12 = 2.812(2). Bond angles (deg): O1−Zr1−O2 = 150.51(6), O1−Zr1−C34 = 98.16(8), O2−Zr1−C34 = 111.20(8), O1−Zr1−C27 = 93.29(8), O2−Zr1−C27 = 90.35(8), C34−Zr1−C27 = 88.33(9), O1−Zr1−N1 = 99.42(6), O2−Zr1−N1 = 83.65(6), C34−Zr1−N1 = 79.80(8), C27−Zr1−N1 = 163.68(8), O1−Zr1−N1′ = 88.93(14), O2−Zr1−N1′ = 92.65(14), C34−Zr1−N1′ = 81.43(15), C27−Zr1−N1′ = 169.74(14), N1−Zr1−N1′ = 10.49(13).

upfield, the pincer $C_{ipso}-H$ proton appears at 4.40 ppm, which corresponds to an aromatic carbon at 113.5 ppm. Adjacent to this proton is the minor isomer resonance at 4.52 ppm. The dibenzyl complex **2** also exhibits an unusual upfield resonance for the $C_{ipso}-H$ proton at 5.17 ppm. Normally this proton resides downfield in the 7.5−8.5 ppm region of the ^{1}H NMR spectrum. Close inspection of the solid-state structure of **9** provides an explanation for the dramatic shift, and Figure 7 depicts a truncated section of **9** that highlights this interaction. The calculated $C_{ipso}-H$ proton points into the center of a benzyl aromatic ring, thus shielding it from the external field and causing the upfield resonance.

If, instead of isolating **9** upon precipitation, the reaction mixture is stirred for 12 h, the second α-picoline equivalent binds and reacts to form the dipyridyl complex [^{t}BuOCHO]-Zr(η^2-(*N,C*)-6-Me-pyridyl)(η^2-(*N,C*-CH_2)-pyrid-2-yl) (**10**) (Scheme 2). Multinuclear NMR spectroscopy and single-crystal X-ray crystallography support the structural assignment. Complex **10** is not stable at ambient temperature in the solid state; the colorless microcrystalline powder turns pink within 2 days. A ^{1}H NMR spectrum of a sample left at ambient temperature in the solid state reveals the presence of the protonated ligand precursor [^{t}BuOCO]H_3 (**1**) and α-picoline. A pentane/diethyl ether solution of **10** cooled to −35 °C in a glovebox freezer results in the formation of an unidentifiable red impurity. However, dissolving **10** in hot pentane and cooling the solution slowly produces crystals suitable for a single-crystal X-ray diffraction experiment as well as some decomposition products. Figure 8 depicts the result of the structural refinement, the figure caption contains pertinent bond lengths and angles, and Table 2 gives the crystal refinement data. Complex **10** contains three unique metallacycles in a C_1-symmetric arrangement: (1) the chelating diphenolate, (2) the η^2-(*N,C*)-6-Me-pyridyl, and (3) the η^2-(*N,C*-CH_2)-pyrid-2-yl.[54,62−65] The inclusion of three metallacycles results in a highly distorted six-coordinate Zr(IV) ion. The highly distorted geometry does not conform to any regular polyhedron. The best description of the geometry is a square pyramid in which the C−N bond of the η^2-(*N,C*)-6-Me-pyridyl, the diphenolate alkoxides, and the N atom of the η^2-(*N,C*-CH_2)-pyrid-2-yl occupy the square plane. The CH_2 group from the η^2-(*N,C*-CH_2)-pyrid-2-yl occupies the apical position, though due to the chelate its position deiviates significantly. Possibly to avoid opposing strong Zr−C trans bonds, the N atoms orient linearly opposite each other (∠N1−Zr−N2 = 172.05(7)°) and force the Zr−C bonds cis (∠C27−Zr1−C38 = 91.06(9)°). In the η^2-(*N,C*)-6-Me-pyridyl three-membered ring the Zr1−N2 and Zr1−C38 distances are 2.2425(18) and 2.230(2) Å, respectively, and the N2−Zr1−C38 angle is 34.82(7)°. These metrics compare well to those of **7** (Zr1−N2 = 2.203(2) Å, Zr1−C39 = 2.253(2) Å, and N1−Zr1−C2 = 34.78(8)°) and the reported [Cp_2Zr(η^2-(*N,C*)-6-Me-pyridyl)(PMe_3)]$^+$ complex[53] (where Zr−N = 2.21(1) Å, Zr−C = 2.29(2) Å, and N−Zr−C = 34.2(7)°). In the η^2-(*N,C*-CH_2)-pyrid-2-yl four-membered ring, a larger N−Zr−C angle appears and the Zr−C bond is appropriately 0.087(3) Å longer (Zr1−C27 = 2.317(3) Å). For comparison, the Zr1−N1 (2.3199(19) Å) distance is significantly shorter than in [Cp_2Zr(η^2(*N,C*-CH_2)-6-Me-pyridyl)]$^+$ (2.407(4) Å)[63] and slightly longer than in [Cp_2Zr-(η^2(*N,C*-CH_2CH_2)-6-Me-pyridyl)]$^+$ (2.303(2) Å).[53]

Retaining C_s symmetry in solution (C_6D_6), the ^{1}H NMR spectrum of **10** reveals a single resonance for the ^{t}Bu protons at 1.05 ppm. A distinct singlet appears at 2.82 ppm for the η^2-(*N,C*-CH_2)-pyrid-2-yl methylene protons, and in the ^{13}C-{^{1}H} NMR spectrum, the corresponding carbon resonates at 43.2 ppm. The methyl group protons on the η^2-(*N,C*)-6-Me-pyridyl ligand resonate as a broad singlet at 1.88 ppm, which is significantly shifted upfield from those of free α-picoline

(62) Kim, Y. H.; Kim, T. H.; Kim, N. Y.; Cho, E. S.; Lee, B. Y.; Shin, D. M.; Chung, Y. K. *Organometallics* **2003**, *22*, 1503.
(63) Beshouri, S. M.; Fanwick, P. E.; Rothwell, I. P.; Huffman, J. C. *Organometallics* **1987**, *6*, 891.
(64) Beshouri, S. M.; Chebi, D. E.; Fanwick, P. E.; Rothwell, I. P.; Huffman, J. C. *Organometallics* **1990**, *9*, 2375.
(65) Bailey, S. I.; Colgan, D.; Engelhardt, L. M.; Leung, W. P.; Papasergio, R. I.; Raston, C. L.; White, A. H. *J. Chem. Soc., Dalton Trans.* **1986**, 603.

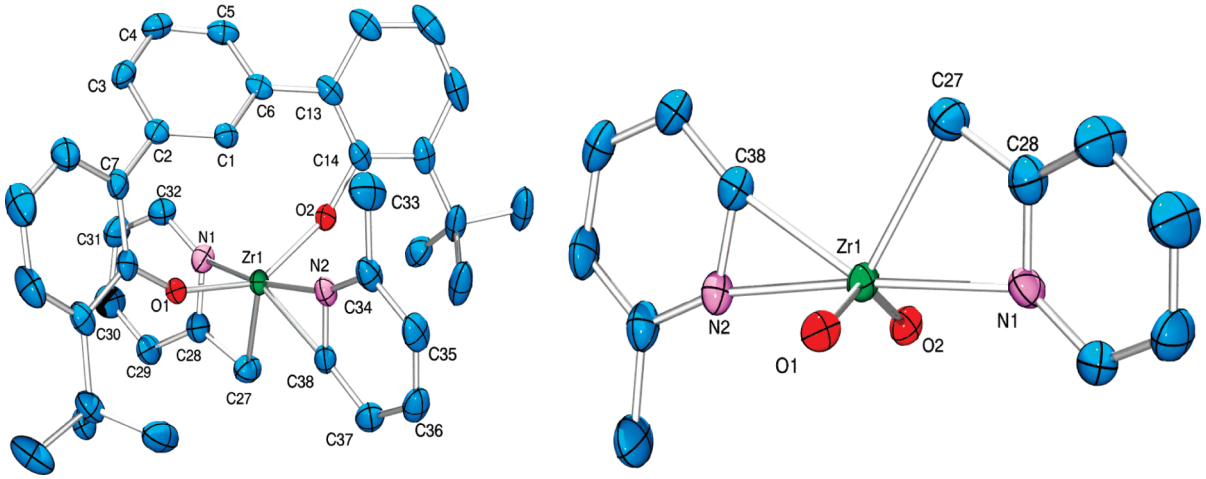

Figure 8. Molecular structure of **10** (left) with ellipsoids drawn at the 50% probability level and hydrogen atoms and solvent molecules (benzene) removed for clarity and the truncated structure of **10** (right) highlighting the Zr(IV) coordination sphere. Selected bond distances (Å): Zr1−O1 = 1.9760(15), Zr1−O2 = 1.9866(15), Zr1−N1 = 2.3199(19), Zr1−N2 = 2.2425(18), Zr1−C27 = 2.317(3), Zr1−C38 = 2.230(2), Zr1−C1 = 2.842(2). Bond angles (deg: O1−Zr1−O2 = 147.18(6), O1−Zr1−C38 = 100.30(7), O2−Zr1−C38 = 98.31(7), O1−Zr1−N2 = 93.92(6), O2−Zr1−N2 = 86.18(6), C38−Zr1−N2 = 34.82(7), O1−Zr1−C27 = 103.08(9), O2−Zr1−C27 = 103.36(9), C38−Zr1−C27 = 91.06(9), N2−Zr1−C27 = 125.70(8), O1−Zr1−N1 = 90.44(6), O2−Zr1−N1 = 86.55(6), C38−Zr1−N1 = 150.26(8), N2−Zr1−N1 = 172.05(7), C27−Zr1−N1 = 59.38(8).

(2.39 ppm) and of **9** (2.19 ppm). With the benzyl groups removed and no aromatic ring to shield it, the diphenolate $C_{ipso}-H$ proton appears in a typical position at 8.98 ppm, though somewhat downfield from **7** (7.11 ppm). Thermolysis of **10** for 12 h in C_6D_6 at 100 °C does not activate the $C_{ipso}-H$ proton to provide the trianionic pincer form of the ligand; instead, the solution turns red. Above 100 °C **10** decomposes rapidly.

Conclusions

In the absence of a σ-donor, the diphenolate complex [^{t}BuOCHO]Zr(CH_2Ph)$_2$ (**2**) converts to the dimer {[^{t}BuOCO]-ZrCH_2Ph}$_2$ (**3**) upon heating. Complex **3** contains a bridging aryloxide ligand from the OCO trianionic pincer, rendering it inert to further derivatization, including no reaction with H_2, CO, or ethylene. The bridging aryloxide indicates the ^{t}Bu group is not bulky enough to prevent dimerization, which is undesirable, especially if this occurs during catalytic processes such as polymerization of alkenes.[7,25] Supporting this contention is the observation that two ligands can bind one Zr ion, exemplified in the synthesis of the bis-diphenolate complex [^{t}BuOCO]$_2$Zr (**6**). The dimerization reaction requires some thermal input (80 °C, 2 h), in contrast to events when σ-donor ligands are present. Addition of THF or PMe_3 promotes the facile loss of toluene and C−H activation of the pincer C_{ipso}-H bond to create the trianionic pincer form of the ligand and the corresponding mononuclear complexes [^{t}BuOCO]Zr$CH_2Ph(L)_2$ (L = PMe_3, **4-PMe$_3$**; L = THF, **5**). What role does the σ-donor play? It is well-known that addition of external nucleophiles to dialkyl complexes promotes α-abstraction resulting in alkylidene formation.[30,66−70] If this occurs, then the pincer $C_{ipso}-H$ bond can add across the resulting M=C double bond. Alternatively, addition of the nucleophile may assist by forcing the benzyl group into a cis position that maximizes orbital alignment for metathesis with the pincer $C_{ipso}-H$ bond. The crystallographically characterized α-picoline complex [^{t}BuOCHO]-Zr(CH_2Ph)$_2$(α-picoline) (**9**) features this precise arrangement. In fact, a recent study by Bercaw et al. indicates both mechanisms are competitive during formation of a titanium dimer analogous to **3**.[25]

The presence of an *o*-C−H bond on py shunts the pincer $C_{ipso}-H$ bond activation, leading to the η^2-pyridinyl complex [^{t}BuOCHO]Zr(CH_2Ph)(η-C_5H_4N)py (**7**). This chemistry can be extended to primary C−H bond activation when α-picoline is the substrate, leading to [^{t}BuOCHO]Zr(η^2(*N,C*)-6-Me-pyridyl)(η^2(*N,C*-CH_2)-pyrid-2-yl) (**10**). Regardless of the mechanism, addition of a σ donor prevents deleterious dimerization and provides a method to convert terphenyl diphenolate ligands into their trianionic form. The σ donors also enable the isolation of monoalkyl complexes supported by trianionic pincer ligands. Exhibition of facile aryl and primary C−H bond activation reactions are compelling; the challenge remains to exploit them in catalytic reactions.

Synthetic Procedures

General Considerations. Unless specified otherwise, all manipulations were performed under an inert atmosphere using standard Schlenk or glovebox techniques. Glassware was oven-dried before use. Pentane, toluene, diethyl ether (Et_2O), tetrahydrofuran (THF), and 1,2-dimethoxyethane (DME) were dried using a GlassContours drying column. Benzene-d_6 and THF-d_8 (Cambridge Isotopes) were dried over sodium−benzophenone ketyl, distilled or vacuum-transferred, and stored over 4 Å molecular sieves. Pyridine was dried over KOH and distilled and stored over 4 Å molecular sieves. Commercially available Zr(CH_2Ph)$_4$ and PMe_3 were used without further purification. [^{t}BuOCO]H_3[28] was prepared according to the literature procedures. NMR spectra were obtained on Varian Mercury Broad Band 300 MHz or Varian Mercury 300 MHz spectrometers. Chemical shifts are

(66) Morton, L. A.; Chen, S. J.; Qiu, H.; Xue, Z. L. *J. Am. Chem. Soc.* **2007**, *129*, 7277.
(67) Schrock, R. R. *Acc. Chem. Res.* **1979**, *12*, 98.
(68) Schrock, R. R.; Fellmann, J. D. *J. Am. Chem. Soc.* **1978**, *100*, 3359.
(69) Mclain, S. J.; Wood, C. D.; Messerle, L. W.; Schrock, R. R.; Hollander, F. J.; Youngs, W. J.; Churchill, M. R. *J. Am. Chem. Soc.* **1978**, *100*, 5962.
(70) Fellmann, J. D.; Rupprecht, G. A.; Wood, C. D.; Schrock, R. R. *J. Am. Chem. Soc.* **1978**, *100*, 5964.

reported in δ (ppm). For ^{1}H and ^{13}C{^{1}H} NMR spectra the solvent resonance was referenced as an internal standard, and for ^{31}P{^{1}H} NMR spectra the 85% H_3PO_4 resonance was referenced as an external standard. Elemental analyses were performed at Complete Analysis Laboratory Inc., Parsippany, NJ.

Synthesis of [^{t}BuOCHO]Zr(CH$_2$Ph)$_2$ (2). A sealable NMR tube was charged with [^{t}BuOCO]H$_3$ (**1**; 46 mg, 0.123 mmol) and benzene-d_6 (0.3 mL) and then frozen (−35 °C). Zr(CH$_2$Ph)$_4$ (56 mg, 0.123 mmol) was dissolved in benzene-d_6 (0.3 mL) and then added to the frozen solution of **1**. The resulting mixture was warmed to 23 °C and then filtered. All volatiles were removed in vacuo to yield **2** as a yellow crystalline solid (70 mg, 88%). ^{1}H NMR (300 MHz, C_6D_6; δ (ppm)): 7.38 (dd, J = 6.1 Hz, 2H, Ar *H*), 7.00−7.02 (m, 3H, Ar *H*), 6.88 (dd, J = 7.6 Hz, 4H, Ar *H*), 6.79 (dd, J = 6.1 Hz, 4H, Ar *H*), 6.66−6.76 (m, 5H, Ar *H*), 6.57−6.59 (m, 1H, Ar *H*), 5.17 (s, 1H, Ar *H*), 3.13 (s, 2H, −C*H*$_2$Ph), 2.72 (s, 2H, −C*H*$_2$Ph), 1.63 (s, 18H, −C(C*H*$_3$)$_3$). ^{13}C{^{1}H} NMR (75.36 Hz, C_6D_6; δ (ppm)): 159.5, 146.7, 138.0, 137.1, 135.7, 133.3, 133.3, 131.6, 131.1, 130.9, 129.7, 129.7, 129.4, 128.9, 128.9, 128.8, 128.0, 126.0, 124.4, 124.2, 121.0, 113.0 (aryl), 66.5 (s, −*C*H$_2$Ph), 65.5 (s, −*C*H$_2$Ph), 35.9 (s, −*C*(CH$_3$)$_3$), 31.5 (s, −C(*C*H$_3$)$_3$). Anal. Calcd for $C_{40}H_{42}O_2Zr$: C, 74.37; H, 6.55. Found: C, 74.35; H, 6.37.

Synthesis of {[^{t}BuOCO]ZrCH$_2$Ph}$_2$ (3). A sealable NMR tube was charged with [^{t}BuOCO]H$_3$ (**1**) (46 mg, 0.123 mmol) and benzene-d_6 (0.3 mL) and then frozen (−35 °C). Zr(CH$_2$Ph)$_4$ (56 mg, 0.123 mmol) was dissolved in benzene-d_6 (0.3 mL) and then added to the frozen solution of **1**. The resulting mixture was warmed to 23 °C and then placed in an 80 °C oil bath for 2 h. The reaction mixture was cooled to room temperature, and all volatiles were removed in vacuo. The crude product was washed two times with cold pentanes, to yield **3** as a pale yellow crystalline solid (40 mg, 59%). ^{1}H NMR (300 MHz, C_6D_6; δ (ppm)): 7.40 (d, J = 7.0 Hz, 1H, Ar *H*), 7.12−7.24 (m, 3H, Ar *H*), 6.79−6.90 (m, 3H, Ar *H*), 6.63 (t, J = 7.8 Hz, 1H, Ar *H*), 6.48 (d, J = 7.3 Hz, 1H, Ar *H*), 6.30 (t, J = 7.5 Hz, 2H, Ar *H*), 6.20 (t, J = 7.3 Hz, 1H, Ar *H*), 6.07 (d, J = 7.0 Hz, 1H, Ar *H*), 2.87 (d, J = 10.1 Hz, 1H, −C*H*$_2$Ph), 2.58 (d, J = 10.1 Hz, 1H, −C*H*$_2$Ph), 1.78 (s, 9H, −C(C*H*$_3$)$_3$), 1.23 (s, 9H, −C(C*H*$_3$)$_3$). ^{13}C{^{1}H} NMR (75.4 Hz, C_6D_6; δ (ppm)): 190.9 (Zr−C$_{pincer}$, 158.0, 151.4, 140.3, 140.2, 140.0, 138.7, 137.5, 136.9, 133.1, 132.9, 131.2, 129.4, 129.1, 126.7, 126.8, 125.6, 125.3, 124.7, 121.1 (aryl), 67.0 (s, −*C*H$_2$Ph), 35.9 (s, −*C*(CH$_3$)$_3$), 35.4 (s, −*C*(CH$_3$)$_3$), 33.5 (s, −C(*C*H$_3$)$_3$), 30.6 (s, −C(*C*H$_3$)$_3$). Anal. Calcd for $C_{33}H_{34}O_2Zr$: C, 71.56; H, 6.19. Found: C, 71.29; H, 6.10.

Synthesis of [^{t}BuOCO]ZrCH$_2$Ph(PMe$_3$)$_2$ (4-PMe$_3$). A sealable NMR tube was charged with [^{t}BuOCO]H$_3$ (**1**; 46 mg, 0.123 mmol) and benzene-d_6 (0.3 mL) and then frozen (−35 °C). Zr(CH$_2$Ph)$_4$ (56 mg, 0.123 mmol) was dissolved in benzene-d_6 (0.3 mL) and then added to the frozen solution of **1**. The resulting mixture was warmed to 23 °C, and then PMe$_3$ (13 μL, 0.246 mmol) was added. The reaction mixture was allowed to stand at 23 °C for 3 h to yield yellow blocks of **4-PMe$_3$** (45 mg, 52%). ^{1}H NMR (300 MHz, C_6D_6; δ (ppm)): 7.60−7.71 (m, 7H, Ar *H*), 7.34 (m, J = 7.6 Hz, 3H, Ar *H*), 7.26 (t, J = 7.6 Hz, 2H, Ar *H*), 6.96 (t, J = 7.8 Hz, 1H, Ar *H*), 6.81 (t, J = 7.3 Hz, 1H, Ar *H*), 2.77 (s, 2H, −C*H*$_2$Ph), 1.67 (s, 18H, −C(C*H*$_3$)$_3$), 0.33 (bs, 18H, -P(C*H*$_3$)$_3$). ^{13}C{^{1}H} NMR (75.36 Hz, C_6D_6; δ (ppm)): 194.8 (s, Zr−C$_{pincer}$), 158.8, 145.2, 142.2, 138.2, 136.1, 130.9, 130.5, 130.1, 128.2, 127.4, 126.0, 124.3, 121.0, 119.9 (aryl), 52.6 (s, −*C*H$_2$Ph), 35.7 (s, −*C*(CH$_3$)$_3$), 30.8 (s, −C(*C*H$_3$)$_3$), 13.0 (dd, J_{PC} = 13.0 Hz, −P(*C*H$_3$)$_3$). ^{31}P{^{1}H} NMR (121 Hz, C_6D_6; δ (ppm)): 31.54 (bs). Anal. Calcd for $C_{39}H_{52}O_2P_2Zr$: C, 66.35; H, 7.42. Found: C, 66.28; H, 7.25.

Synthesis of [^{t}BuOCO]ZrCH$_2$Ph(THF)$_2$ (5). A sealable NMR tube was charged with [^{t}BuOCO]H$_3$ (**1**; 46 mg, 0.123 mmol) and benzene-d_6 (0.3 mL) and then frozen (−35 °C). Zr(CH$_2$Ph)$_4$ (56 mg, 0.123 mmol) was dissolved in benzene-d_6 (0.3 mL) and then added to the frozen solution of **1**. The resulting mixture was warmed to 23 °C to form **2** in situ. The reaction solution was frozen again, THF (18 mg, 0.246 mmol, 2 equiv) was added, and the mixture was slowly warmed to 23 °C. All volatiles were removed in vacuo to yield **5** as a pale yellow crystalline solid (80 mg, 93%). ^{1}H NMR (300 MHz, C_6D_6; δ (ppm)): 7.70 (m, 4H, Ar *H*), 7.43 (d, J = 7.6 Hz, 2H, Ar *H*), 7.31 (dd, J = 7.8 Hz, 2H, Ar *H*), 7.05 (t, J = 7.8 Hz, 1H, Ar *H*), 6.93 (m, 3H, Ar *H*), 6.72 (bm, 2H, Ar *H*), 6.46 (t, J = 6.7 Hz, 1H, Ar *H*), 3.48 (bs, 8H, −OC*H*$_2$), 2.89 (s, 2H, −C*H*$_2$Ph), 1.76 (s, 18H, −C(C*H*$_3$)$_3$), 0.96 (s, 8H, −C*H*$_2$). ^{13}C{^{1}H} NMR (75.4 Hz, C_6D_6; δ (ppm)): 189.9 (s, Zr−C$_{pincer}$), 157.6, 144.1, 138.4, 135.7, 130.5, 130.1, 130.1, 129.7, 127.5, 126.5, 126.0, 125.3, 123.8, 119.8 (aryl), 72.3 (s, −OCH$_2$), 58.8 (s, −*C*H$_2$Ph), 35.7 (s, −*C*(CH$_3$)$_3$), 31.1 (s, −C(*C*H$_3$)$_3$), 25.4 (s, −*C*H$_2$). Anal. Calcd for $C_{41}H_{50}O_4Zr$: C, 70.54; H, 7.22. Found: C, 70.46; H, 7.06.

Synthesis of [^{t}BuOCHO]$_2$Zr (6). A sealable NMR tube or a vial was charged with [^{t}BuOCO]H$_3$ (**1**; 46 mg, 0.123 mmol) and benzene (0.3 mL) and then frozen (−35 °C). Zr(CH$_2$Ph)$_4$ (28 mg, 0.062 mmol) was dissolved in benzene (0.3 mL) and then added to the frozen solution of **1**. The resulting mixture was slowly warmed to 23 °C. Analytically pure colorless crystalline solid or single crystals of **6** were obtained from the reaction mixture (35 mg, 68%, based on Zr starting material). Anal. Calcd for $C_{52}H_{56}O_4Zr$: C, 74.69; H, 6.75. Found: C, 74.89; H, 6.60.

Synthesis of [^{t}BuOCHO]ZrCH$_2$Ph(η^2-C$_5$H$_4$N)py (7). A sealable NMR tube was charged with [^{t}BuOCO]H$_3$ (**1**; 46 mg, 0.123 mmol) and benzene-d_6 (0.3 mL) and then frozen (−35 °C). Zr(CH$_2$Ph)$_4$ (56 mg, 0.123 mmol) was dissolved in benzene-d_6 (0.3 mL) and then added to the frozen solution of **1**. The resulting mixture was warmed to 23 °C to form **2** in situ. The reaction solution was frozen again, pyridine (20 mg, 0.246 mmol, 2 equiv) was added, and the mixture was slowly warmed to 23 °C. The progress of the reaction was monitored periodically by ^{1}H NMR spectroscopy to determine the end point. Typically the reaction was complete after 1−2 h. All volatiles were removed in vacuo, and the crude product was washed with cold pentanes (3 × 2 mL) to yield **7** as a colorless crystalline solid (60 mg, 69%). ^{1}H NMR (300 MHz, C_6D_6, 10 °C; δ (ppm)): 9.30 (bs, 1H, Ar *H*), 8.83 (bs, 1H, Ar *H*), 8.30 (d, J = 5.2 Hz, 2H, Ar *H*), 7.80 (dd, J = 6.4 Hz, J = 7.3 Hz, 2H, Ar *H*), 7.61 (bs, 1H, Ar *H*), 7.39 (d, J = 7.9 Hz, 2H, Ar *H*), 7.31 (d, J = 2.2 Hz, 2H, Ar *H*), 7.11 (s, 1H, Ar *H*), 7.06 (d, J = 6.4 Hz, 2H, Ar *H*), 7.00 (s, 1H, Ar *H*), 6.95 (t, J = 7.9 Hz, 2H, Ar *H*), 6.87−6.90 (m, 2H, Ar *H*), 6.84 (s, 1H, Ar *H*), 6.63 (dd, J = 7.6 Hz, J = 7.9 Hz, 2H, Ar *H*), 6.19 (t, J = 6.4 Hz, 2H, Ar *H*), 2.79 (bs, 2H, −C*H*$_2$Ph), 1.30 (s, 18H, −C(C*H*$_3$)$_3$). ^{13}C{^{1}H} NMR (75.36 Hz, C_6D_6, 10 °C; δ (ppm)): 201.1 (s, Zr−C$_{pincer}$), 160.0, 155.2, 150.8, 149.9, 146.9, 142.4, 137.7, 137.3, 136.9, 136.5, 133.6, 132.2, 130.5, 129.8, 129.6, 127.5, 126.5, 125.0, 124.7, 123.8, 120.1, 119.8, 117.4 (aryl), 57.8 (s, −*C*H$_2$Ph), 35.5 (s, −*C*(CH$_3$)$_3$), 30.4 (s, −C(*C*H$_3$)$_3$). Anal. Calcd for $C_{43}H_{44}N_2O_2Zr$: C, 72.53; H, 6.23; N, 3.93. Found: C, 72.42; H, 6.18; N, 3.82.

Synthesis of [^{t}BuOCO]Zr(η^2-C$_5$H$_4$N)(py)$_2$ (8). A sealable NMR tube was charged with [^{t}BuOCO]H$_3$ (**1**; 46 mg, 0.123 mmol) and benzene-d_6 (0.3 mL) and then frozen (−35 °C). Zr(CH$_2$Ph)$_4$ (56 mg, 0.123 mmol) was dissolved in benzene-d_6 (0.3 mL) and then added to the frozen solution of **1**. The resulting mixture was warmed to 23 °C to form **2** in situ. The reaction solution was frozen again, pyridine (30 mg, 0.369 mmol, 3 equiv) was added, and the mixture was warmed to 23 °C. The resulting solution was heated to 50 °C for 1 h. All volatiles were removed in vacuo to provide a light brown solid that was washed with cold pentanes (3 × 2 mL) to yield **8** as a colorless crystalline solid (80 mg, 93%). ^{1}H NMR (300 MHz, C_7D_8; δ (ppm)): 8.73 (bs, 4H, Ar *H*), 7.83 (d, J = 4.9 Hz, 1H, Ar *H*), 7.73 (t, J = 1.2 Hz, 1H, Ar *H*), 7.71 (t, J = 1.2 Hz, 1H, Ar *H*), 7.68 (d, J = 7.6 Hz, 3H, Ar *H*), 7.27 (dd, J = 1.5 Hz, J = 7.6 Hz, 2H, Ar *H*), 7.24 (s, 1H, Ar *H*), 7.19 (dd, J = 7.9 Hz, J = 7.6 Hz, 1H, Ar *H*), 6.89 (dd, J = 7.9 Hz, J = 7.6 Hz, 2H, Ar *H*), 6.72 (bs, 1H, Ar *H*), 6.60 (bs, 2H, Ar *H*), 6.30 (bs, 4H, Ar *H*), 1.37 (s, 18H, −C(C*H*$_3$)$_3$). ^{13}C{^{1}H} NMR (75.36 Hz, C_7D_8; δ (ppm)): 207.9 (s, Zr−*C*$_{py}$), 188.2 (s, Zr−*C*$_{pincer}$), 157.4, 150.3,

144.1, 142.0, 137.1, 136.8, 136.5, 136.1, 129.4, 129.2, 128.5, 128.4, 126.8, 125.8, 125.6, 124.5, 123.7, 123.5, 119.0 (aryl), 35.0 (s, $-C(CH_3)_3$), 30.2 (s, $-C(CH_3)_3$). Anal. Calcd for $C_{41}H_{41}N_3O_2Zr$: C, 70.45; H, 5.91; N, 6.01. Found: C, 70.64; H, 6.09; N, 5.87.

Synthesis of [^{t}BuOCHO]Zr(CH_2Ph)$_2$(α-picoline) (9). A sealable NMR tube or a vial was charged with [^{t}BuOCO]H_3 (**1**; 46 mg, 0.123 mmol) and benzene-d_6 (0.3 mL) and then frozen (−35 °C). $Zr(CH_2Ph)_4$ (56 mg, 0.123 mmol) was dissolved in benzene-d_6 (0.3 mL) and then added to the frozen solution of **1**. The resulting mixture was warmed to 23 °C to form **2** in situ. The reaction solution was frozen again, α-picoline (24 μL, 0.246 mmol, 2 equiv) was added, and the mixture was warmed to 23 °C. Analytically pure, dark yellow blocks of **9** precipitated after 10 min from the reaction mixture, and all volatiles were removed in vacuo for 12 h to provide a yellow powder (80 mg, 88%). There are two isomers of **9** (**9A**, 87% and **9B**, 13%) at −25 °C. Data for **9A** are as follows. ^{1}H NMR (300 MHz, $CDCl_3$ at −25 °C; δ (ppm)): 8.31 (bs, 1H, Ar *H*), 7.50 (dd, *J* = 4.6 Hz, *J* = 4.9 Hz, 2H, Ar *H*), 7.40 (s, 5H, Ar *H*), 6.96−7.01 (m, 5H, Ar *H*), 6.73 (t, *J* = 8.6 Hz, 3H, Ar *H*), 6.65 (d, *J* = 7.0 Hz, 4H, Ar *H*), 6.41 (dd, *J* = 6.4 Hz, *J* = 7.0 Hz, 1H, Ar *H*), 6.31 (t, *J* = 7.3 Hz, 2H, Ar *H*), 4.40 (s, 1H, Ar *H*), 2.97 (s, 2H, $-CH_2Ph$), 2.56 (s, 2H, $-CH_2Ph$), 2.19 (bs, 3H, $-CH_3$), 1.75 (s, 18H, $-C(CH_3)_3$). $^{13}C\{^1H\}$ NMR (75.36 Hz, $CDCl_3$ at −25 °C; δ (ppm)): 158.5, 145.3, 139.7, 136.9, 133.0, 131.5, 129.9, 129.2, 128.8, 128.5, 128.4, 128.0, 127.4, 127.3, 125.8, 125.4, 121.2, 120.7, 120.6, 120.1, 113.5 (aryl), 68.9 (s, $-CH_2Ph$), 68.1 (s, $-CH_2Ph$), 35.6 (s, $-C(CH_3)_3$), 31.2 (s, $-C(CH_3)_3$), 24.6 (s, $-CH_3$). Data for **9B** are as follows. ^{1}H NMR (300 MHz, $CDCl_3$ at −25 °C; δ (ppm)): 4.52 (s, 1H, Ar *H*), 3.12 (bs, 3H, $-CH_3$), 2.73 (s, 2H, $-CH_2Ph$), 2.63 (s, 2H, $-CH_2Ph$), 1.75 (s, 18H, $-C(CH_3)_3$). Anal. Calcd for $C_{46}H_{49}NO_2Zr$: C, 74.75; H, 6.68; N, 1.90. Found: C, 74.59; H, 6.57; N, 1.92.

Synthesis of [^{t}BuOCHO]Zr(η^2(*N,C*)-6-Me-pyridyl)(η^2(*N,C*-CH_2)-pyrid-2-yl) (10). A sealable NMR tube or a vial was charged with [^{t}BuOCO]H_3 (**1**; 46 mg, 0.123 mmol) and benzene-d_6 (0.3 mL) and then frozen (−35 °C). $Zr(CH_2Ph)_4$ (56 mg, 0.123 mmol) was dissolved in benzene-d_6 (0.3 mL) and then added to the frozen solution of **1**. The resulting mixture was warmed to 23 °C to form **2** in situ. The reaction solution was frozen again, α-picoline (24 μL, 0.246 mmol, 2 equiv) was added, and the mixture was warmed to 23 °C. The reaction mixture was allowed to stand or was stirred at room temperature for 12 h to form **10**. All volatiles were removed in vacuo, and the crude compound was recrystallized from hot pentanes (50 mg, 65%). ^{1}H NMR (300 MHz, benzene-d_6; δ (ppm)): 8.98 (bs, 1H, Ar *H*), 7.89 (bs, 1H, Ar *H*), 7.41 (d, *J* = 5.8 Hz, 1H, Ar *H*), 7.38 (d, *J* = 5.8 Hz, 1H, Ar *H*), 7.34 (t, *J* = 1.8 Hz, 2H, Ar *H*), 7.32 (d, *J* = 1.8 Hz, 1H, Ar *H*), 7.22 (dd, *J* = 1.5 Hz, *J* = 1.8 Hz, 2H, Ar *H*), 7.14 (dd, *J* = 6.7 Hz, *J* = 7.3 Hz, 1H, Ar *H*), 6.81−6.91 (m, 5H, Ar *H*), 6.47 (d, *J* = 7.3 Hz, 1H, Ar *H*), 6.15 (dd, *J* = 6.7 Hz, *J* = 7.0 Hz, 1H, Ar *H*), 2.82 (s, 2H, $-CH_2$), 1.88 (bs, 3H, $-CH_3$), 1.05 (s, 18H, $-C(CH_3)_3$). $^{13}C\{^1H\}$ NMR (75.36 Hz, benzene-d_6; δ (ppm)): 199.8 (s, Zr$-C_{\alpha\text{-picoline}}$), 167.4, 160.6, 154.4, 153.7, 147.2, 146.4, 139.0, 138.0, 137.8, 133.4, 133.3, 132.2, 132.1, 129.4, 129.3, 128.9, 128.5, 128.2, 127.6, 127.5, 127.4, 125.5, 124.3, 123.0, 119.3, 117.2, 115.3 (aryl), 43.2(s, $-CH_2$), 35.3 (s, $-C(CH_3)_3$), 30.2 (s, $-C(CH_3)_3$), 21.8 (s, $-CH_3$).

NMR Tube Reaction: Formation of [^{t}BuOCO]ZrCH_2Ph(PMe_2Ph) (4-PMe_2Ph). A sealable NMR tube was charged with [^{t}BuOCO]H_3 (**1**; 23 mg, 0.062 mmol) and benzene-d_6 (0.3 mL) and then frozen (−35 °C). $Zr(CH_2Ph)_4$ (28 mg, 0.062 mmol) was dissolved in benzene-d_6 (0.3 mL) and then added to the frozen solution of **1**. The resulting mixture was warmed to 23 °C, and PMe_2Ph (17.5 μL, 0.123 mmol) was then added, and the mixture was allowed to stand at 23 °C for 10 min. ^{1}H NMR (300 MHz, C_6D_6; δ (ppm)): 7.75 (d, *J* = 7.6 Hz, 2H, Ar *H*), 7.66 (dd, *J* = 4.5 Hz, *J* = 1.5 Hz, 2H, Ar *H*), 7.37 (overlapping doublets, *J* = 7.5 Hz, 4H, Ar *H*), 7.1 - 6.7 (m, Ar *H*), 6.53 (t, *J* = 7.3 Hz, 1H, Ar *H*), 2.55 (s, 2H, $-CH_2Ph$), 1.52 (s, 18H, $-C(CH_3)_3$), 0.60 (bs, 6H, $-P(CH_3)_2Ph$). $^{13}C\{^1H\}$ NMR (75.36 Hz, C_6D_6; δ (ppm)): 194.6 (s, Zr$-C_{pincer}$), 158.7, 145.2, 141.3, 137.8, 136.4, 131.1, 129.7, 129.2, 128.9, 127.3, 125.8, 124.4, 120.0 (aryl), 53.9 (s, $-CH_2Ph$), 35.6 (s, $-C(CH_3)_3$), 30.9 (s, $-C(CH_3)_3$), 12.2 (bs, $-P(CH_3)_2Ph$). Note: the aromatic carbons of the Zr-PMe_2Ph group are broadened due to exchange with free PMe_2Ph and could not be assigned. $^{31}P\{^1H\}$ NMR (121 Hz, C_6D_6; δ (ppm)): −18.6 (bs).

Acknowledgment. A.S.V. thanks UF, NSF CAREER (No. CHE-0748408), the Camille and Henry Dreyfus Foundation, and The Alfred P. Sloan Foundation for financial support of this work. K.A.A. thanks UF and the NSF (No. CHE-0821346) for funding the purchase of X-ray equipment.

Supporting Information Available: Text, figures, tables, and CIF files giving full experimental procedures, NMR spectra, and X-ray crystallographic details. This material is available free of charge via the Internet at http://pubs.acs.org.